



SINTEF

Report

Geomagnetically induced currents in a Norwegian transformer station

Comparison of two years of GIC- and magnetometer measurements

Author(s):

Kristian Solheim Thinn, Olve Mo and Magnar Gullikstad
Johnsen (UiT Norges Arktiske Universitet)

Report No:

2021:01449 - Unrestricted

Client:

NVE (Norges Vassdrags- og Energidirektorat)

Report

Geomagnetically induced currents in a Norwegian transformer station

Comparison of two years of GIC- and magnetometer measurements

KEYWORDS

Geomagnetically induced currents (GIC)
Magnetometers
Geomagnetic fields
Measurements
Hall effect sensors
Space weather
Solar Storms
Geomagnetic storms
Power grid

VERSION

3.0

DATE

2022-08-04

AUTHORS

Kristian Solheim Thinn, Olve Mo and Magnar Gullikstad Johnsen (UIT Norges Arktiske Universitet)

CLIENT

NVE (Norges Vassdrags- og Energidirektorat)

CLIENT'S REFERENCE

Astri Gillund

PROJECT NO.

502001693

NO. OF PAGES

66

SUMMARY

This report considers measurements of geomagnetically induced current (GIC) and comparison to recorded variations in the geomagnetic field (dB/dt).

The GIC-sensors were installed in the neutral point of a 420 kV transformer located in Mid-Norway in 2019. The magnetometers (for dB/dt) are also located in Mid-Norway, but at another location. Recordings up to December 2021 are presented in this report. The maximum recorded GIC and dB/dt was about +/- 60 A and 14 nT/s, respectively.

From linear regression, GIC is approximated to 3 times dB/dt, where GIC is measured in amps and dB/dt in nT/s. GIC is always lower than 7 times dB/dt based on the dataset with day-max values (699 points).

PREPARED BY

Kristian Solheim Thinn

SIGNATURE

Kristian Solheim Thinn

Kristian Solheim Thinn (Aug 8, 2022 19:59 GMT+2)

CHECKED BY

Olve Mo

SIGNATURE

Olve Mo

Olve Mo (Aug 9, 2022 07:53 GMT+2)

APPROVED BY

Dag Eirik Nordgård

SIGNATURE

Dag Eirik Nordgård

Dag Eirik Nordgård (Aug 9, 2022 08:34 GMT+2)

REPORT NO.

2021:01449

ISBN

978-82-14-07705-6

CLASSIFICATION

Unrestricted

CLASSIFICATION THIS PAGE

Unrestricted

Document history

VERSION	DATE	VERSION DESCRIPTION
1.0	2021-12-16	Issued for review
2.0	2022-05-11	Final version.
3.0	2022-08-04	Final version. Updated typo in Section 5.1.

Table of contents

1	INTRODUCTION	4
2	SUMMARY AND CONCLUSIONS.....	5
3	EQUIPMENT FOR GIC RECORDINGS	7
3.1	Installation of sensors and control cabinet.....	7
3.2	GIC-sensors	10
3.3	PC, data logger and internet	11
3.4	Other equipment	11
4	RECORDING OF GIC.....	12
4.1	Overview	12
4.2	Recordings 2019-2021	14
4.3	Recordings 27.09.2019 and 28.09.2020	17
4.4	Adjusted GIC-offset.....	20
5	RECORDING OF GEOMAGNETIC FIELDS.....	22
5.1	Introduction	22
5.2	Recordings 2019-2021	23
5.2.1	Geomagnetic field.....	23
5.2.2	Variation in magnetic field	25
6	COMPARISON BETWEEN GIC AND dB/dT.....	27
6.1	Recordings 2019-2021	27
6.2	Recordings 27.09.2019, 28.09.2020 and 03.11.2021	29
6.3	Correlation GIC and dB/dt.....	31
7	REFERENCES.....	35
APPENDIX A: BROCHURES GIC-SENSORS		36
APPENDIX B: CALIBRATION CERTIFICATEs GIC-SENSORS		43
APPENDIX C: DOCUMENTATION OTHER EQUIPMENT		38

1 INTRODUCTION

Geomagnetic storms may induce quasi-DC currents (geomagnetically induced currents, GIC) in the transmission grid that may damage critical components, destabilize the power supply and result in long-duration power outages. Transformers that have a solid bonded earth connection, mostly found at the highest voltage levels with long transmission lines, are most vulnerable. The challenge is related to saturation of the transformers that may cause increased use of reactive power, voltage drop in the grid and overheating of the transformers.

Four GIC-sensors were installed in the neutral point of a 420 kV transformer in Mid-Norway. The sensors have recorded GIC for two years between 2019 and 2021. In this report, the installation and measurement set-up is detailed (Section 3), while results from recordings are given in Section 4.

An aim of the study has been to explore the relationship between GIC and variation in the geomagnetic fields (dB/dt). In Norway, Tromsø Geophysical Observatory operates a network of magnetometers to monitor Earth's magnetic field. Data from the instrument located at Rørvik (also located in Mid-Norway), have been made available for this study. Samples are taken twice every second and saved as 10 second averages. Recordings of variation in geomagnetic fields are given in Section 5, while the comparison between the recordings are given in Section 6. A section of future work is added in the end of Section 2.

To fully understand the severity of each geomagnetic storm, a correlation between the dB/dt and level of GIC in the transformers and system impact (voltage level, harmonics, reactive power) is needed. This is not a part of this report.

A technical report about measures to handle risks and consequences related to geomagnetic induced currents in the Norwegian power grid was issued in 2021, [1]. It is written by SINTEF on commission by The Norwegian Water Resources and Energy Directorate (NVE).

A few other measurement set-ups for GIC are given in [2], [3], [4] and [5].

2 SUMMARY AND CONCLUSIONS

Introduction (Section 1)

Geomagnetic storms may induce quasi-DC currents (geomagnetically induced currents, GIC) in the transmission grid that may damage critical components, destabilize the power supply and result in long-duration power outages. An aim of this work has been to develop a relationship between the GIC and variation in the geomagnetic fields (dB/dt) for a specific transformer station.

Equipment for and recording of GIC (Sections 3 and 4)

Four GIC-sensors were installed in the neutral point of a 420 kV transformer in Mid-Norway. Two GIC-sensors were purchased from each of the two vendors Dynamic Rating and Advanced Power Technologies. One has low range (~±/− 45A), the other high range (~±/− 500 A). The data presented in this report is recorded momentarily every 15 seconds between 10. September 2019 and 16. November 2021. Data has been recorded in about 700 days. Most of the recorded GIC was between 0 and 10 A. At one instance (in November 2021), about 60-70 A was measured. About 30-40 A was measured two separate days and about 20-30 A was measured six separate days.

Recording of geomagnetic fields (Section 5)

A network of magnetometers, for local measurements of the Earth's magnetic field, are placed throughout Norway. Data from these instruments are available from Tromsø Geophysical Observatory, a part of UiT – The Arctic University of Norway. In this report, the data from the magnetometer in Rørvik is used. The data are measured every 10 seconds. Two measurements are done every second, and it is the average that is saved.

For the magnetic field, the north component dominates. However, for the dB/dt, the geographic orientation of the field is not evident. From September 2019 to November 2021, there are about three instances with dB/dt greater than 10 nT/s. There are about ten instances with dB/dt greater than 5 nT/s.

Comparison between GIC and dB/dt (Section 6)

It is evident that there is a correlation between GIC and dB/dt. Each of the variables fluctuate at the same time instances. However, the magnitude and shape has not the same clear correlation.

The correlation between GIC and dB/dt has been calculated based on linear regression. The dataset day-maximum values (699 days) and hour-maximum values (16 515 hours) are evaluated. The measured data, that has an orientation 3-7° north, is used in the two first formulas. The regression shows that GIC for this location can be estimated by the formula below. The variation (R^2) is 0.76.

$$GIC [A_{dc}] = 3 \cdot \frac{d}{dt} B_{3-7^\circ \text{ North}} \left[\frac{nT}{s} \right]$$

It seems to be a maximum GIC for a given recorded dB/dt. The formula is given below for dataset with day-maximum GIC and dB/dt.

$$GIC [A_{dc}] < 7 \cdot \frac{d}{dt} B_{3-7^\circ \text{ North}} \left[\frac{nT}{s} \right]$$

When comparing dB/dt in north and east direction, none of the components dominate. This indicates that transmission lines with east-west orientation are as vulnerable to GIC as transmission lines oriented north-south. The trend is valid at the location of this specific transformer where GIC is measured and assumes that the electrical field is distributed similar as dB/dt. Local variations in the geological conditions can result in different conclusions at other locations.

By projecting (orienting) the measured geomagnetic field to 0, 15, 30, 45, 60, 75, 90° north (90° north is east), it is found that GIC correlates better to dB/dt at an angle of 45°. R^2 is 0.82. The transmission lines south and north of the transformer station has an orientation of roughly 15° easterly from north. Since dB/dt does not dominate in any direction, it is likely that the maximum correlation for 45 degrees is due to a non-uniform conductivity in the crust

Future work

More data points at higher GIC (>20 A) are needed to increase the accuracy of the relationship between GIC vs. dB/dt at these higher GICs. It is forecasted that solar activity will increase in the coming years, and this should be taken advantage of.

The primary driver of GIC is the geoelectric field, not the geomagnetic field. Therefore, the correlation between GIC and the geoelectric field is assumed to be better than between GIC and dB/dt. Many methods with varying complexity exist to estimate the geoelectric field. The simplest method, assuming the magnetic field variation to be a planar wave incident on the ground, is basically found by integrating dB/dt backwards in time, where recent measurement points are weighted more than older ones. One of the unknowns in the equation is the electrical conductivity in soil that makes it challenging to estimate GIC from dB/dt only. However, when a correlation between GIC and the geomagnetic field is found, the exact value of the soil conductivity (and other parameters) is not needed. The correlation is only valid at the locations where the measurements are taken.

By developing a network model of the grid (in respect to GIC, such as done in [6]) the GIC in an area can be estimated in real-time based on variation in the geoelectrical field. The variation in the geoelectrical field should be calibrated against measurements of GIC.

3 EQUIPMENT FOR GIC RECORDINGS

3.1 Installation of sensors and control cabinet

The GIC-equipment was installed in a 420 kV transformer station in Mid-Norway 10. September 2019. Personnel from NVE, Statnett and SINTEF were present. The four GIC sensors are seen as black and red clamps on the transformer earth busbar in Figure 3-1. The neutral was also threaded through a regular hall effect transformer, as seen in Figure 3-2. The control cabinet is seen in Figure 3-3 and Figure 3-4. In Figure 3-5, a single line diagram of key components is given.



Figure 3-1: Four GIC-sensors (2 black and 2 red) on transformer neutral. Regular hall effect sensor in grey box, see Figure 3-2.



Figure 3-2: Neutral of transformer thread through a regular hall effect sensor (blue). Also a heater (black).

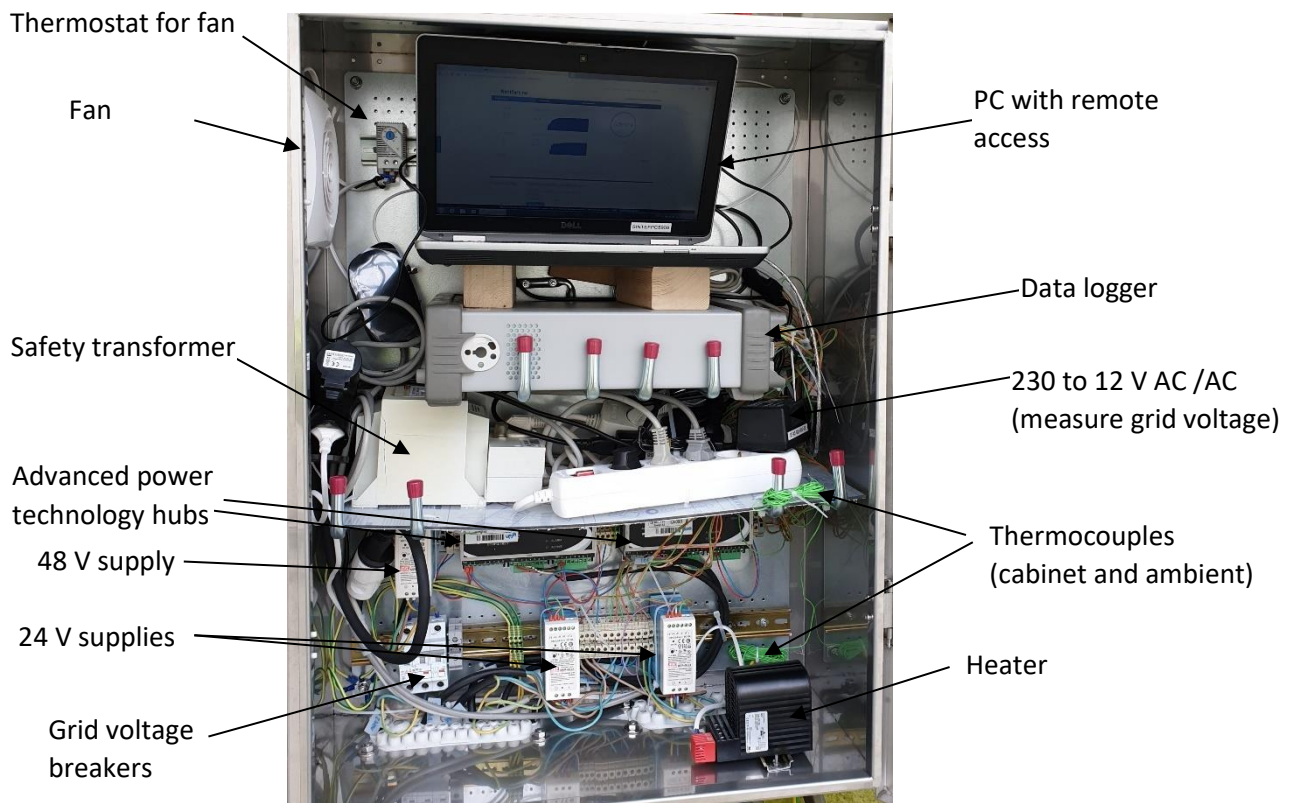


Figure 3-3: Inside control cabinet.

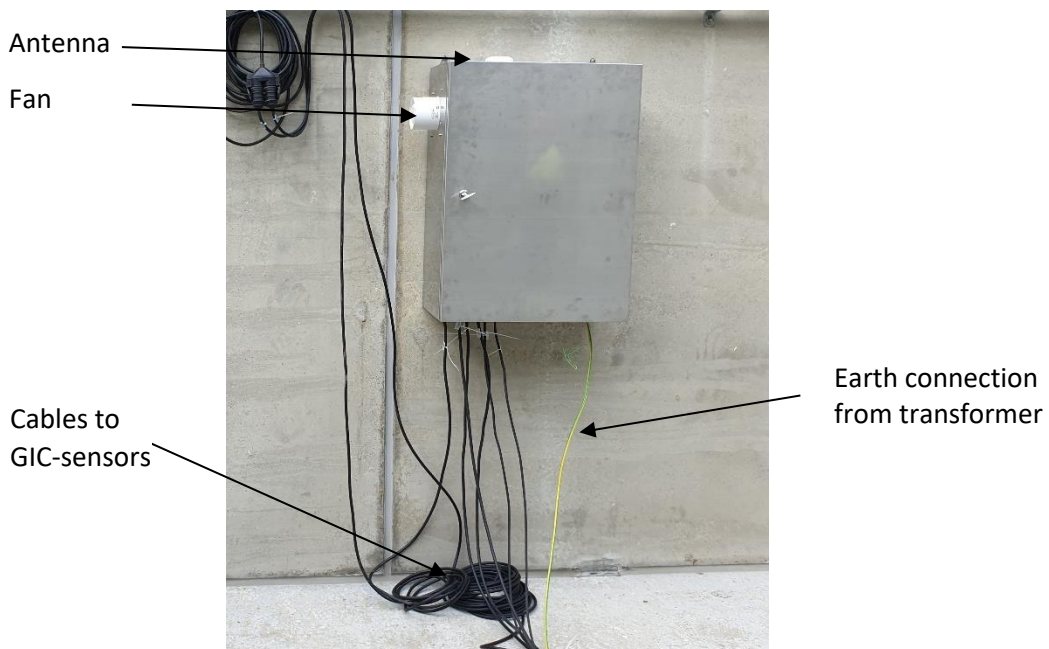


Figure 3-4: Outside control cabinet.

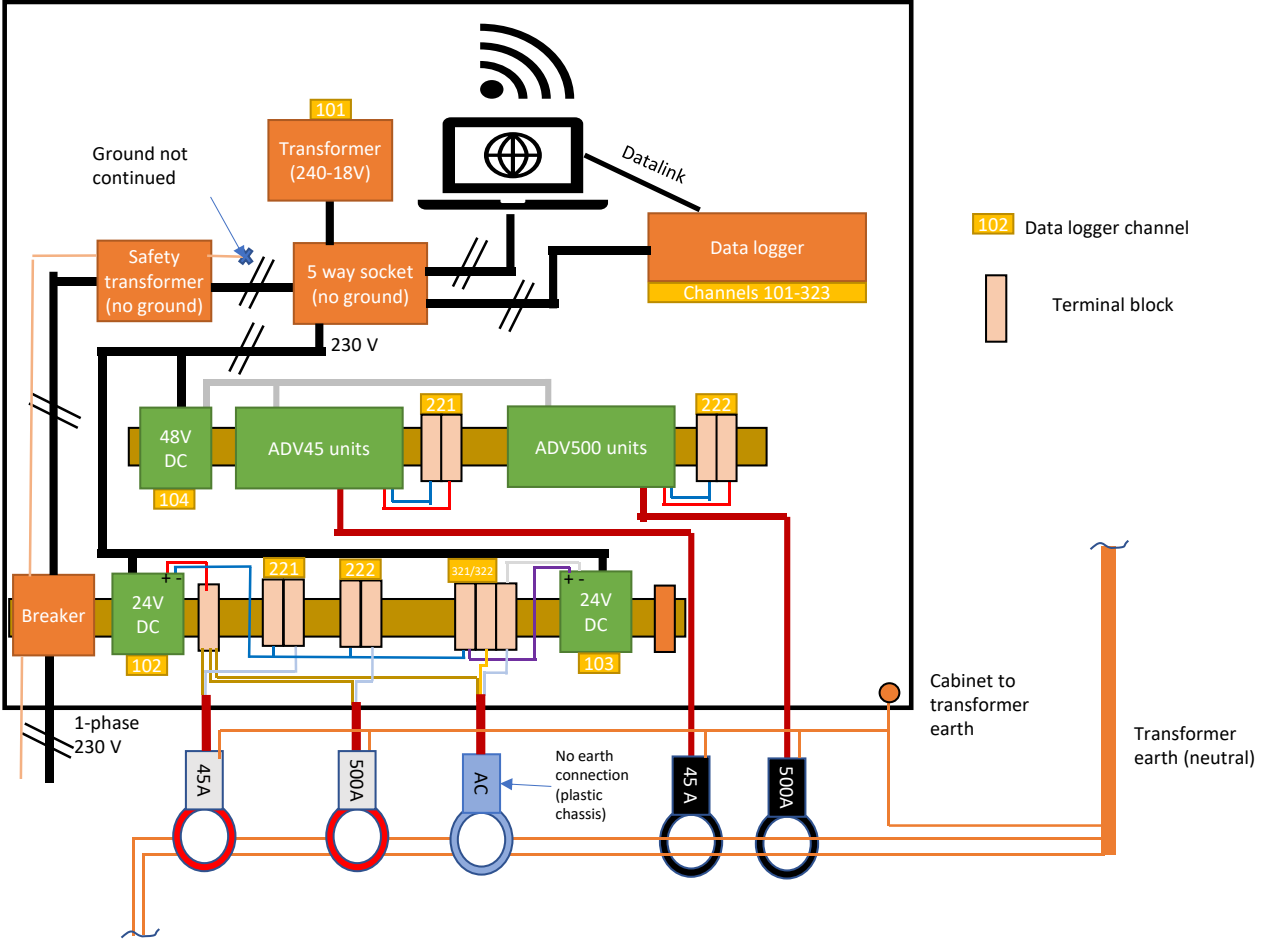


Figure 3-5: Line diagram inside control cabinet of key components.

3.2 GIC-sensors

Two GIC-sensors were purchased from each of the two vendors Dynamic Rating and Advanced Power Technologies. They are all split core hall effect sensors with low pass filters that blocks higher frequencies than a few Hz. One sensor from each vendor has a range of +/- 500 A, while the other has a range of about 45 A. In Appendix A, sales brochures/datasheets are added. The price of each sensor was 2 000-3 000 USD.

Each of the sensors give a 4-20 mA DC-current output signal to the data logger, representing the measured GIC. For the sensors from Dynamic Rating, the signal is given directly from the sensor itself. It is powered by a 24 V DC source. For the Advanced Power Technologies equipment, the sensor is connected to a hub that is powered by a 48 V DC-source. From the hub, a 4-20 mA signal is given. See Figure 3-6 for pictures.

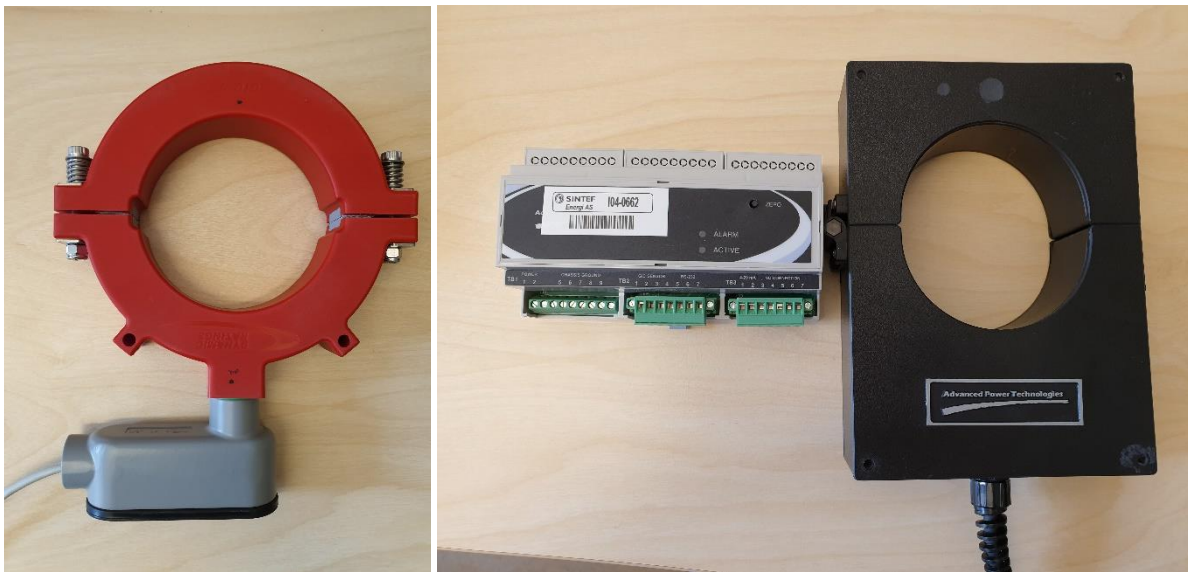


Figure 3-6: GIC sensor from Dynamic Rating (left) and hub and GIC sensor from Advanced Power Technologies (right).

The sensors were calibrated (3 off) or tested (1 off) at vendors site before shipment in 2019. The calibration was tested in a small test setup at SINTEF. The data logger originally used the SINTEF-calibration results. However, in this report, the numbers are transformed to represent the vendor/fabric calibration¹. See Appendix B for calibration certificates. The formula in Table 3-1 gives the GIC current [A_{dc}], where x [A_{dc}] is the measured signal from GIC-sensors (4-20 mA).

Table 3-1: Calibration data and ID for the GIC sensors.

GIC-sensor	SINTEF calibration	Fabric calibration	SINTEF-ID
Dynamic Ratings +/- 37 A	4630,0x – 55.4674	4630,0x – 55,4674	I04-0659
Dynamic Rating +/- 500A	57020,0x – 683.858	57020,0x – 684,240	I04-0660
Advanced Power Tech. +/- 45A	5624.297x – 67.0941	5624,297x – 67,4941	I04-0662
Advanced Power Tech. +/- 500A	62577.59x – 749.852	62577,59x – 749,852	I04-0661

¹ The SINTEF calibration showed more correspondence to a test current that was applied in the lab. However, when the sensors were installed on the 420 kV transformer, an offset in the readings were seen. As the vendor has a defined accuracy with their calibration, it was decided to use their calibration.

In addition to the dedicated GIC-sensors, a regular hall effect sensor, LEM 1005-S, was installed. A reason for installing this was its low cost, about 200 USD. As there are no low pass filters, the entire AC+DC-signal was measured. The hypothesis was that GIC is most relevant for a high DC-component (>50A) and that the error in reading from the AC-component (few amps) would be acceptable. The datasheet is added in Appendix C.

3.3 PC, data logger and internet

The datalogger was of the type Agilent 34970A from Agilent Technologies (SINTEF-ID G05-0190). The datalogger recorded momentarily with a sampling frequency of 15 seconds. A 15 second sampling rate was considered acceptable as reported GIC events normally lasts for at least some minutes. The instrument only allows for momentarily readings (no intermediate processing). The GIC-sensors have built-in low pass filters. The recordings are time instant values. The PC connected to the datalogger was a Dell Latitude E6430 (SINTEF-ID SINTEFPC5908), using recording software Benchlink Data Logger 3. The PC was accessible remotely through the software TeamViewer. The time of the PC may be a few minutes different from actual time, as the automatic built-in correction did not work properly. A mobile broadband unit (ZYXEL WAH7608 before replaced by Avantech ICR-1601 LTE industrial router summer 2020) was connected to the Smarteq 3G/4G boat antenna. Due to various down-time, the recording was stopped and started every about 2 weeks. The broadband unit was rebooted about once a month. See Appendix C for datasheets.

3.4 Other equipment

Other instruments are given in Table 3-2. Only the safety transformer has SINTEF-ID: B01-0610.

Table 3-2: Other equipment installed.

Instrument	Function	Data
Safety transformer	Galvanic separation of all equipment from power grid	Noratel LF-460 ISO F 460 VA
24 V voltage source (x2)	Operating GIC-sensors from Dynamic Rating and hall effect sensors	Mean Well MDR-60-24 24V/2.5A
48 V voltage source	Operating GIC-sensor hub from Advanced Power Technologies	Mean Well MDR-60-48 48V/1.25A
Measurement transformer	For measurement of grid voltage	Mascot type 8810 230V – 18 V AC (1 V = 10.45V)
Control cabinet	Contain instruments	Stainless steel IP65 cabinet SF 806030 800 x 600 x 300
Thermostat for fan	Keep temperatures during summer	Stego KTS 011 0-60°C
Fan	Keep temperatures during summer	Flexit silent eco 100 standard
Cable	Between sensors and cabinet	Rubber cable H07RN-F ANTITWIN 3G1,5
Thermocouples	Measure cabinet and ambient temperature	K-type
Heaters	Keep temperature in winter (5-25°C)	CSF 060 Touch-Safe Heater 06001.0-00

4 RECORDING OF GIC

4.1 Overview

Various voltages and currents were recorded by the instruments, see Table 4-1. For grid voltage (channel 101) and AC current measured by LEM (channel 321), it is the RMS value that is measured by the instrument.

Table 4-1: Recorded parameters.

Channel	Parameter	Symbol and unit
-	Universal time. It can be some minutes deviation.	dd.mm.yyyy hh:mm:ss
101	Grid voltage in cabinet	Vgrid [V _{ac}] (RMS)
102	Voltage of 24V DC source (1)	V24_1 [V _{dc}]
103	Voltage of 24V DC source (2)	V24_2 [V _{dc}]
104	Voltage of 48V DC source	V48 [V _{dc}]
105	Temperature in control cabinet	Tin [°C]
106	Temperature outside control cabinet (ambient)	Tout [°C]
121	Current measured by low range (~+/-45A) GIC sensor from Dynamic Rating	Idyn45 [A _{dc}]
122	Current measured by high range (~+/-500A) GIC sensor from Dynamic Rating	Idyn500 [A _{dc}]
221	Current measured by low range (~+/-45A) GIC sensor from Advanced Power Technologies	Iadv45 [A _{dc}]
222	Current measured by high range (~+/-500A) GIC sensor from Dynamic Rating	Iadv500 [A _{dc}]
321	AC Current measured by LEM	I_LEM_ac [A _{ac}] (RMS)
322	DC Current measured by LEM	I_LEDM_dc [A _{dc}]

As will be seen in the next sections, there were an offset in the recorded values. The recordings were adjusted as given in Table 4-2. The offset is added in the post processing of data in all relevant graphs from Section 4.4.

Table 4-2: Time period for adjustment of offset of GIC sensors. Applied to graphs from Section 4.4.

Time [dd-mm-yyyy hh:mm:ss]	Idyn45 [A]	Idyn500 [A]	Iadv45 [A]	Iadv500 [A]
10-09-2019 12:14:02 (start) to 24-09-2019 07:48:47	0.6343	2.6032	1.6710	2.1582
24-09-2019 07:49:02 to 01-10-2019 07:52:32	1.7547	4.1030	3.1409	3.7253
06-10-2019 01:57:30 to 13-12-2019 07:34:07	1.5852	3.7431	2.4924	3.0537
06-02-2020 09:10:59 to 16-11-2021 13:16:06 (end)	0.3644	2.3992	1.4177	1.9870

There were some down-time of the equipment. Most of the instances were due to lost connection between PC and data logger. In winter 2019/2020, the 48 V source was overloaded, i.e. voltage dropped. At the same time, the LEM gave very high readings before it became corrupt/broken. After this, the 48 V source have been stable. Thus, the readings from the LEM are only for a few months and will be presented, but not discussed further. The period with down-time, lasting for at least a day are given below:

- 02.10.2019-05.10.2019 (3 days)
- 23.10.2019-30.10.2019 (7 days)
- 02.11.2019-05.11.2019 (3 days)
- 14.12.2019-05.02.2020 (53 days)
- 06.05.2020-13.05.2020 (7 days)
- 02.10.2020
- 14.04.2021-19.04.2021 (5 days)
- 07.07.2021-18.07.2021 (11 days)
- 02.10.2021-03.10.2021 (2 days)

The total number of recordings are:

- 4.0 mill (15 sec interval) – about 64 million data points for the 12 channels
- 16 515 (combined to hour interval)
- 699 (combined to day interval)

4.2 Recordings 2019-2021

In this section, an overview of all recordings is given. These are split in two figures: September 2019 to October 2020 (Figure 4-2) and October 2020 to 2021 (Figure 4-3).

In 2019/2020, the grid voltage varies between 230 and 245 V, which is fine for the instruments. The two 24 V DC sources are very stable, apart from a singularity in end of November 2019. The temperature in the cabinet varies in general between 5 and 20 °C in the winter and between 20 and 40°C in the summer. For the 48 V DC-source, the output varies more than the 24V source. It is also noticeable that the source is temperature dependent. As the hubs from Advanced Power Technologies has some range in accepted voltage, it is reason to believe that the variation does largely influence the GIC-readings. The accuracy has not further been discussed. There are only a few periods were recorded GIC is more than 10 A. The measurements of the GIC-sensors should be fluctuating around zero. However, the offset of the GIC varied by a few amps during the record period. A definite reason is not found. It can be error in measurement equipment and/or a combination with any adjustment/connections in the power grid. In Section 4.4, graphs with adjusted offset are presented.

The period 2020/2021 is similar as 2019/2020 for most recordings. It is noticeable that the voltage of one of the 24V DC sources decreases from 24 V to 23.8 V. There is not seen any significant error in the readings of the dynamic rating +/- 45A sensor that is connected. In 2020/2021, there are about five times as many periods with GIC-current more than 20 A compared to in 2020/2019. The highest recorded GIC was in November 2021, around 60-70 A on three GIC-sensors and some above 100 A on the 500A sensor from Advanced Power Technologies.

The major number of recordings (~4 mill) are of GIC less than 10 A. Around 1000-3000 recordings (depending on GIC-sensor) are between 10 and 20 A, and only a few higher than 60 A. Many of the highest recordings are from the same event in November 2021.

The low-cost hall effect sensor (without low pass filter) that was installed shows the same magnitude in DC reading as the more expensive GIC-sensors. See Figure 4-4 (compared to GIC in Figure 4-2). The AC and DC component have the same signal to the recorder. As there is no filter, the measured DC signal can be anywhere on the AC-curve. It did however break down after some month in service. The reason for the breakdown is not known.

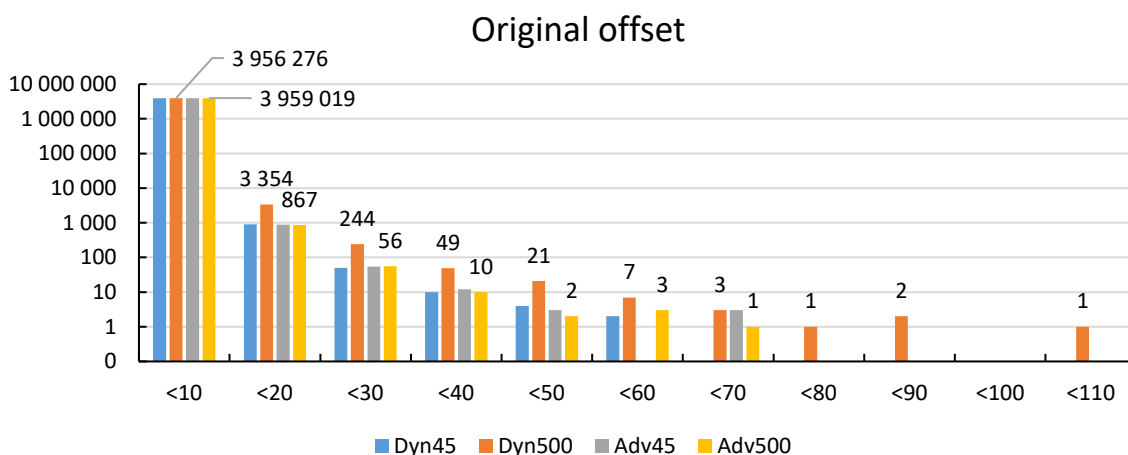


Figure 4-1: Number of measurements at different current with recorded offset from GIC-sensors.

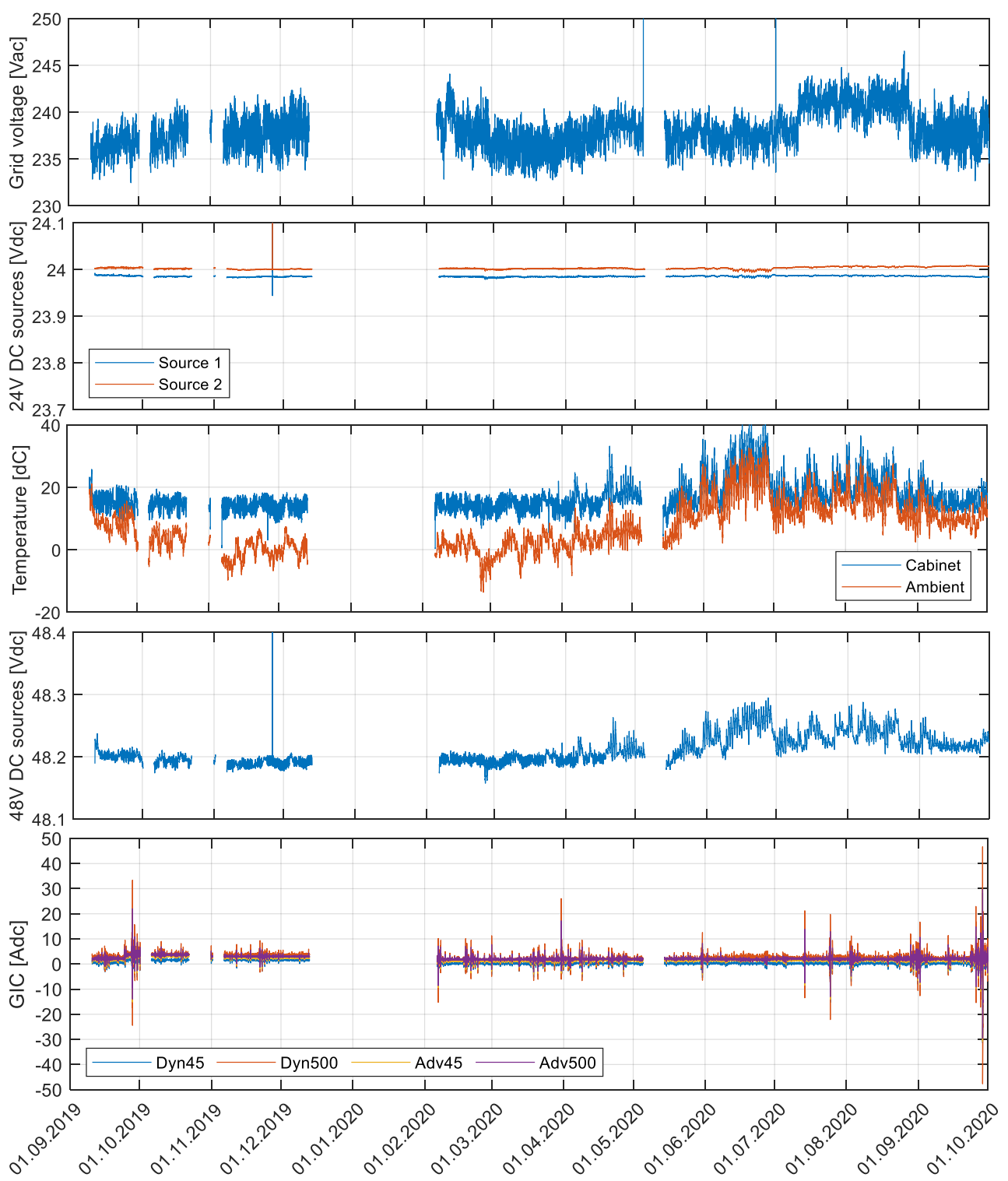


Figure 4-2: Recordings in 2019/2020 of grid voltage, 24 and 48 V DC source voltage, temperature in control cabinet and ambient temperature, and GIC.

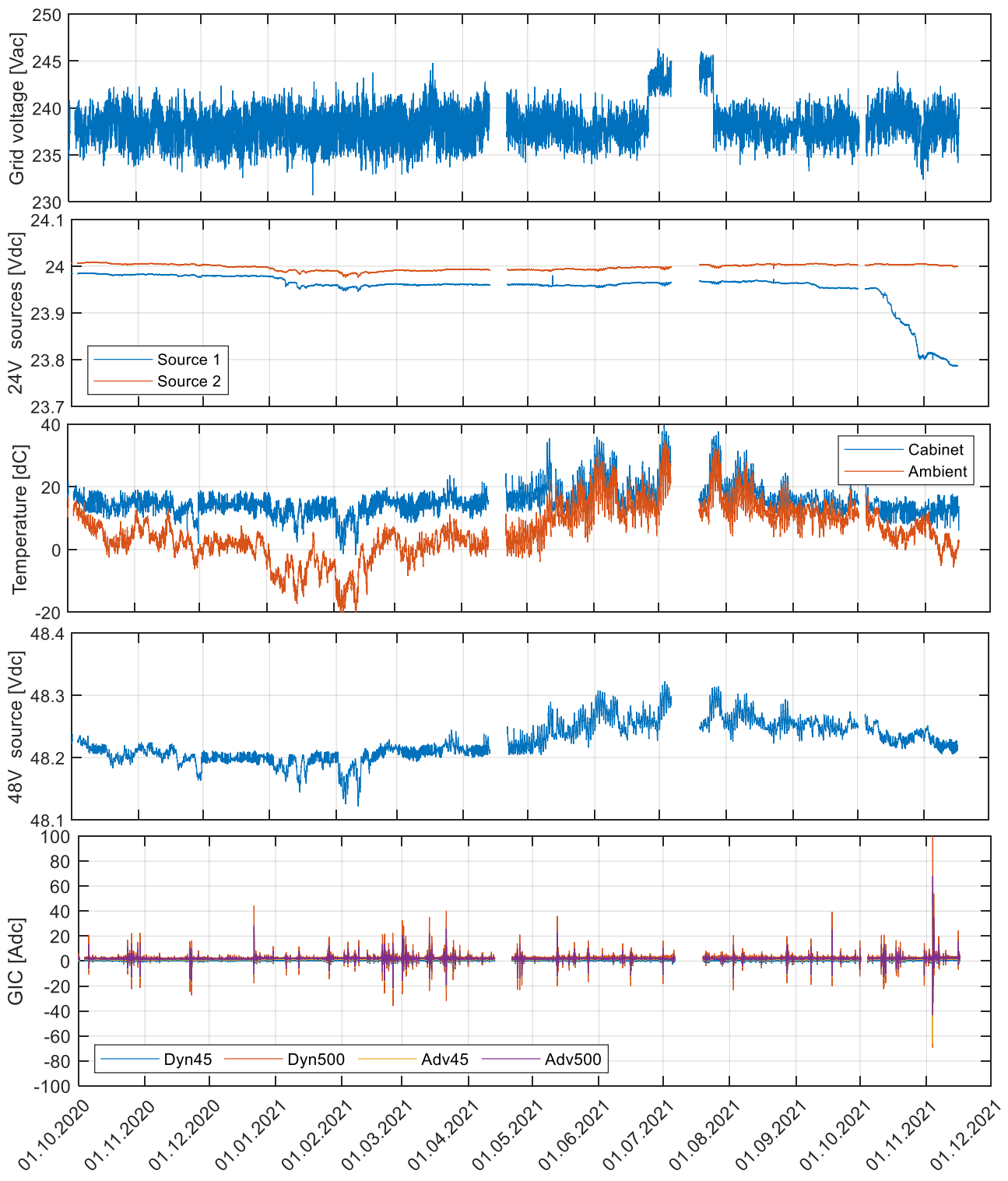


Figure 4-3: Recordings in 2019/2020 of grid voltage, 24 and 48 V DC source voltage, temperature in control cabinet and ambient temperature, and GIC.

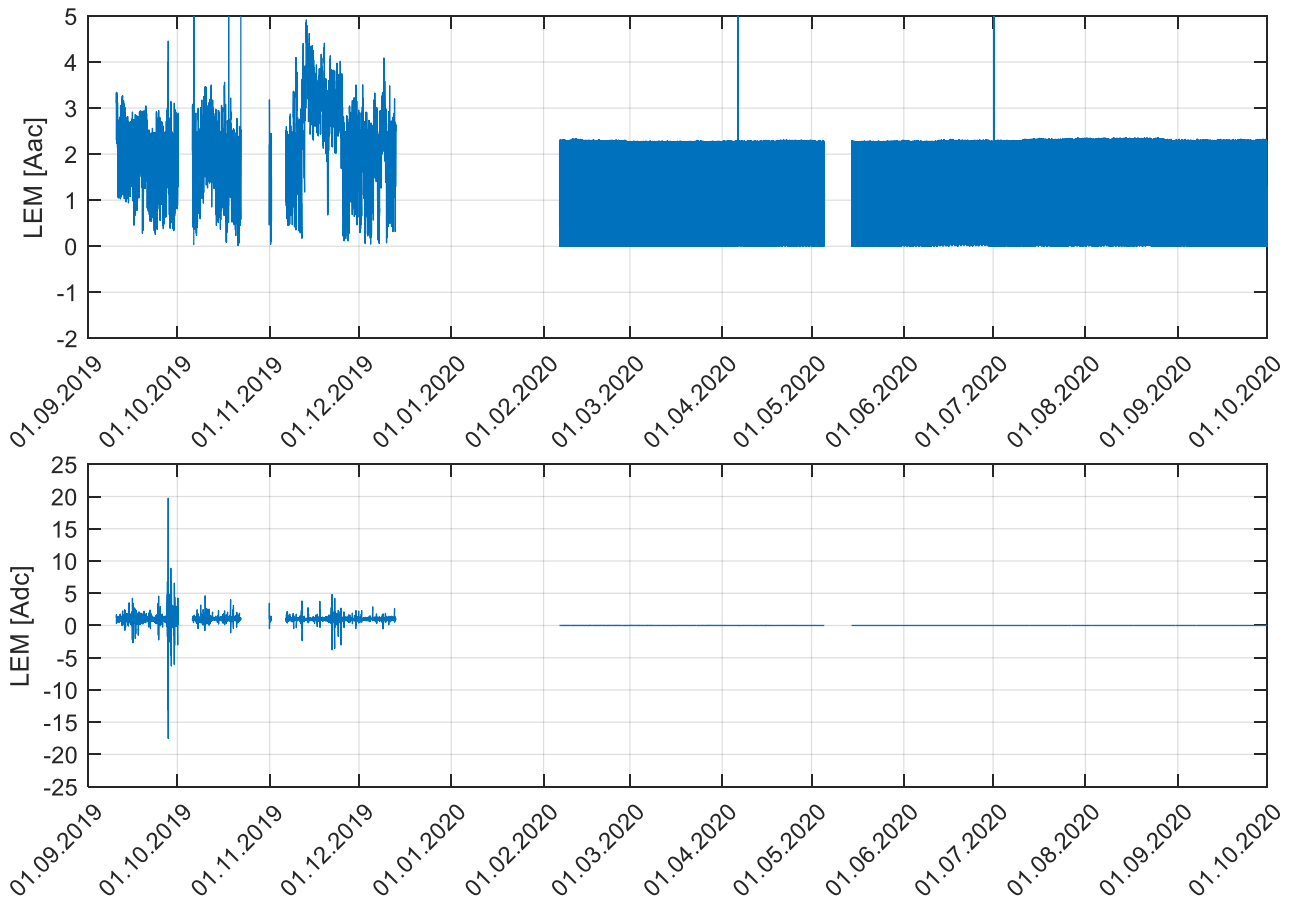


Figure 4-4: Recordings of AC current (upper plot) and DC current (lower plot) from LEM hall effect sensor in 2019/2020. It broke down before February 2020. Note that recording the AC current is measured RMS, while the DC current is instantaneous values. The two channels on the data logger have the same signal from the LEM sensor.

4.3 Recordings 27.09.2019 and 28.09.2020

In this section, the two GIC incidents 27.09.2019 and 28.09.2020 are considered. It is interesting to see how the GIC behaviour is in a time-segment and if this affects any of the other recorded values.

On 27.09.2019, a GIC of about 35 A was measured, see Figure 4-5. A few fluctuations are seen, but the main event is at 22:30. This event lasts for a few minutes. No correlation is seen to measured temperature or voltage from the DC supplies. There is no noticeable correlation to the grid voltage.

About one year later, the 28.09.2020, a GIC of about 50 A was measured, see Figure 4-6. Also here, a few fluctuations are seen in the hours after the main event (18:30). As for 2019, no correlation is seen to measured temperature or voltage from the DC supplies. There seem to be some distortion in grid voltage also at 18:30, that implies that there is a small correlation to the grid voltage. Similar correlation is less prominent at the events around 22:00, but it is also difficult to compare as there is a sudden drop in grid voltage. This could be from adjustment of a transformer tap, or due to the GIC that gives more reactive consumption and consequently a lower voltage.

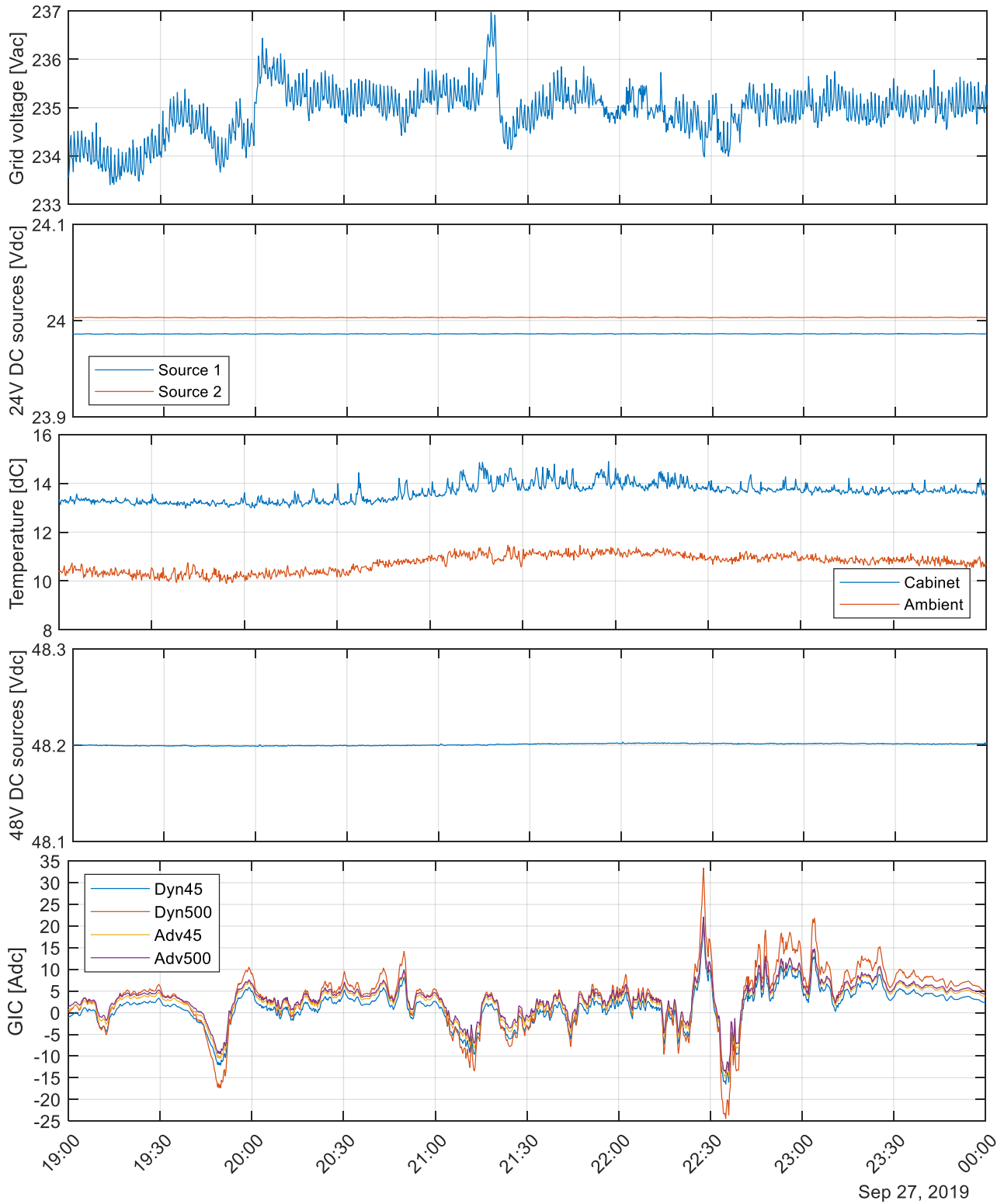


Figure 4-5: Recordings 27.09.2019 of grid voltage, 24 and 48 V DC source voltage, temperature in control cabinet and ambient temperature, and GIC.

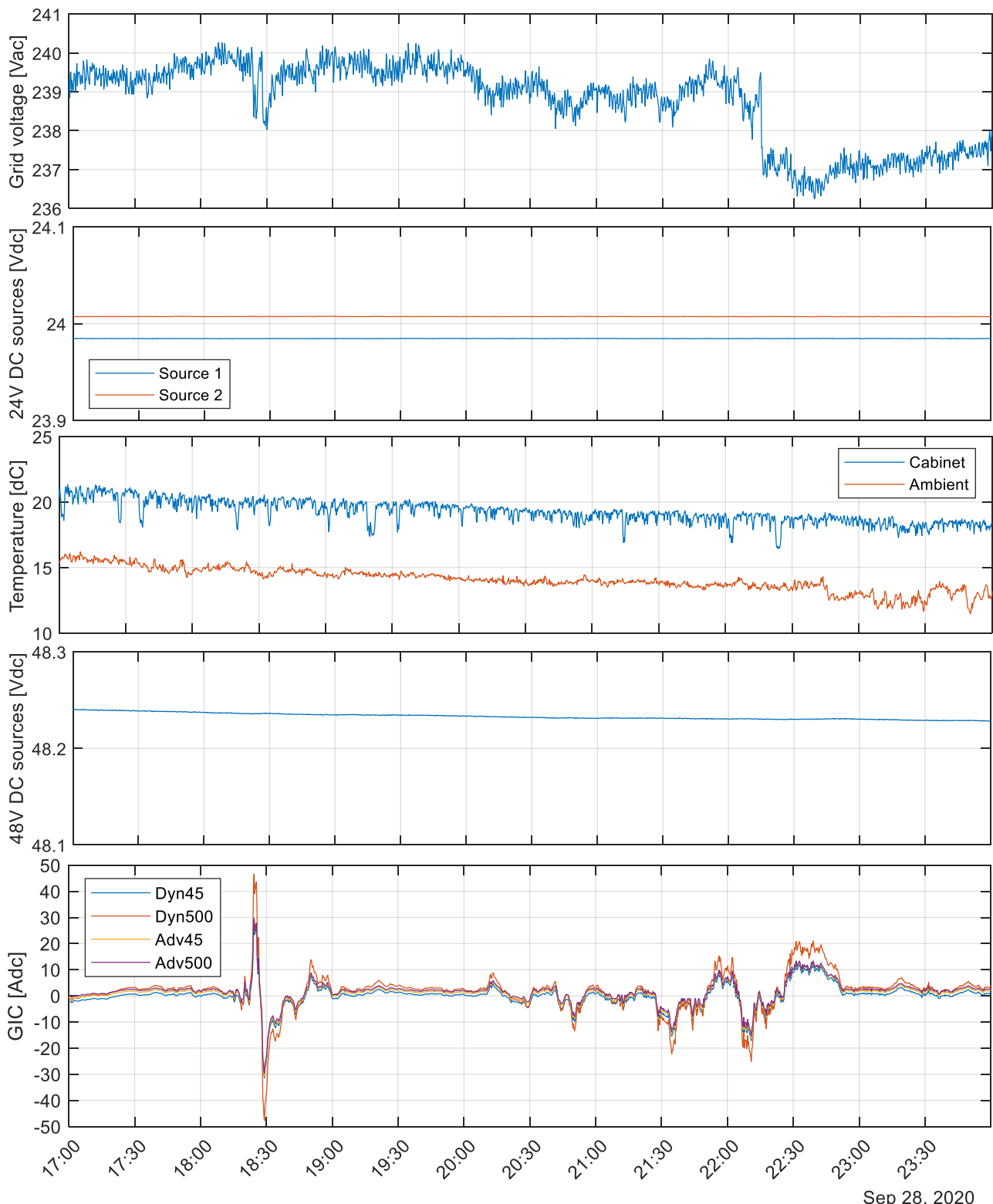


Figure 4-6: Recordings 28.09.2020 of grid voltage, 24 and 48 V DC source voltage, temperature in control cabinet (Tin) and ambient temperature (Tout), and GIC (Adc).

4.4 Adjusted GIC-offset

As indicated in the previous sections, there is an offset in the recorded GIC. In this section, adjustment of the offset is presented. The offset is modified as specified in Table 4-2. The adjustment corresponds to the median in the recorded values in the time periods.

In Figure 4-7 and Figure 4-8, the recordings without offset adjustment, and with offset adjustments are given. As expected, when adjusting the offset, the recorded GIC fluctuates more around zero. In Figure 4-9, the number of recordings with 10A-interval is seen. This is similar to Figure 4-1.

Also, an overview with recordings with 10 A-interval is given for a data set where only the maximum day-value is included, see Figure 4-10. This shows that the many high GIC recordings (<60 A) from Figure 4-9 happened the same day. For the 500A sensor from advanced power technologies, there was one day with GIC between 60 and 70 A, two days with GIC between 30 and 40 A, and 6 days with GIC between 20 and 30 A.

In Section 6, the offset adjusted values are used.

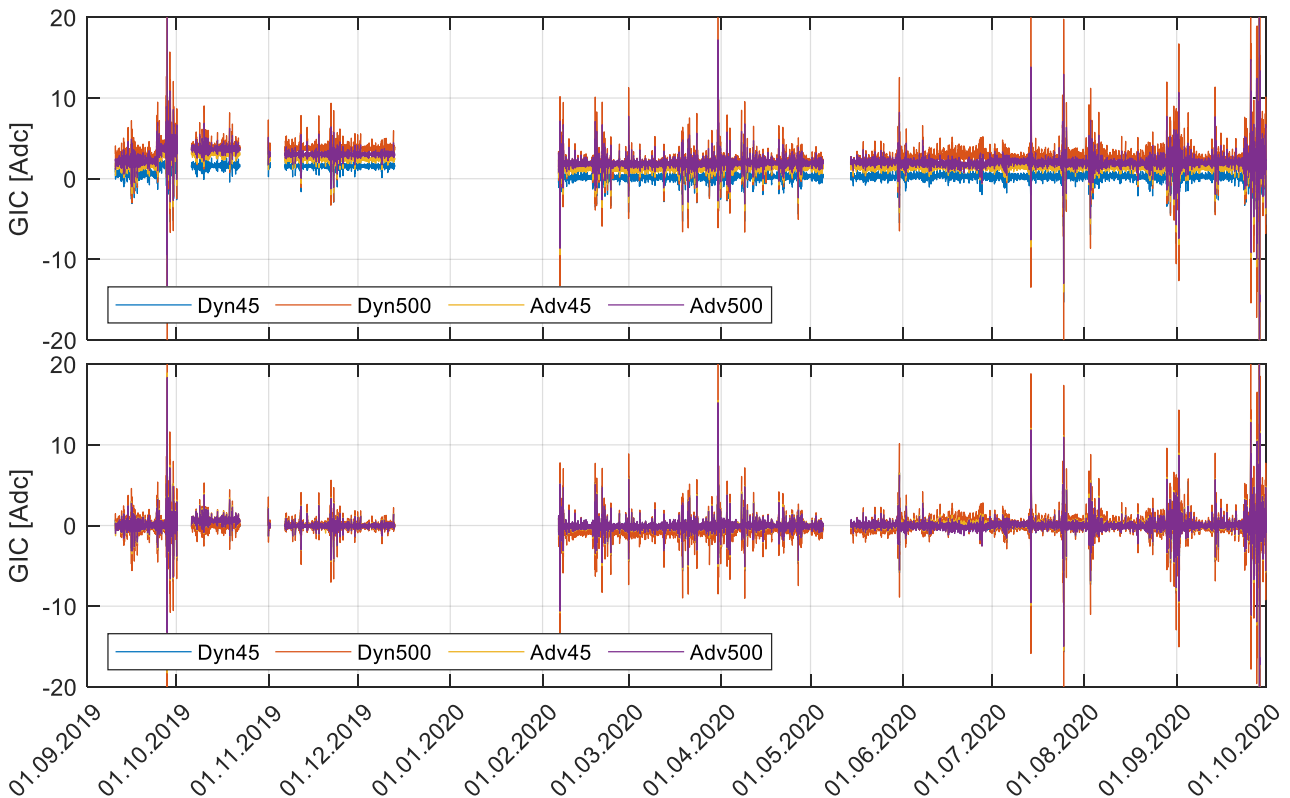


Figure 4-7: Measured GIC in 2019/2020 as recorded by data logger (upper) and offset-adjusted (lower).

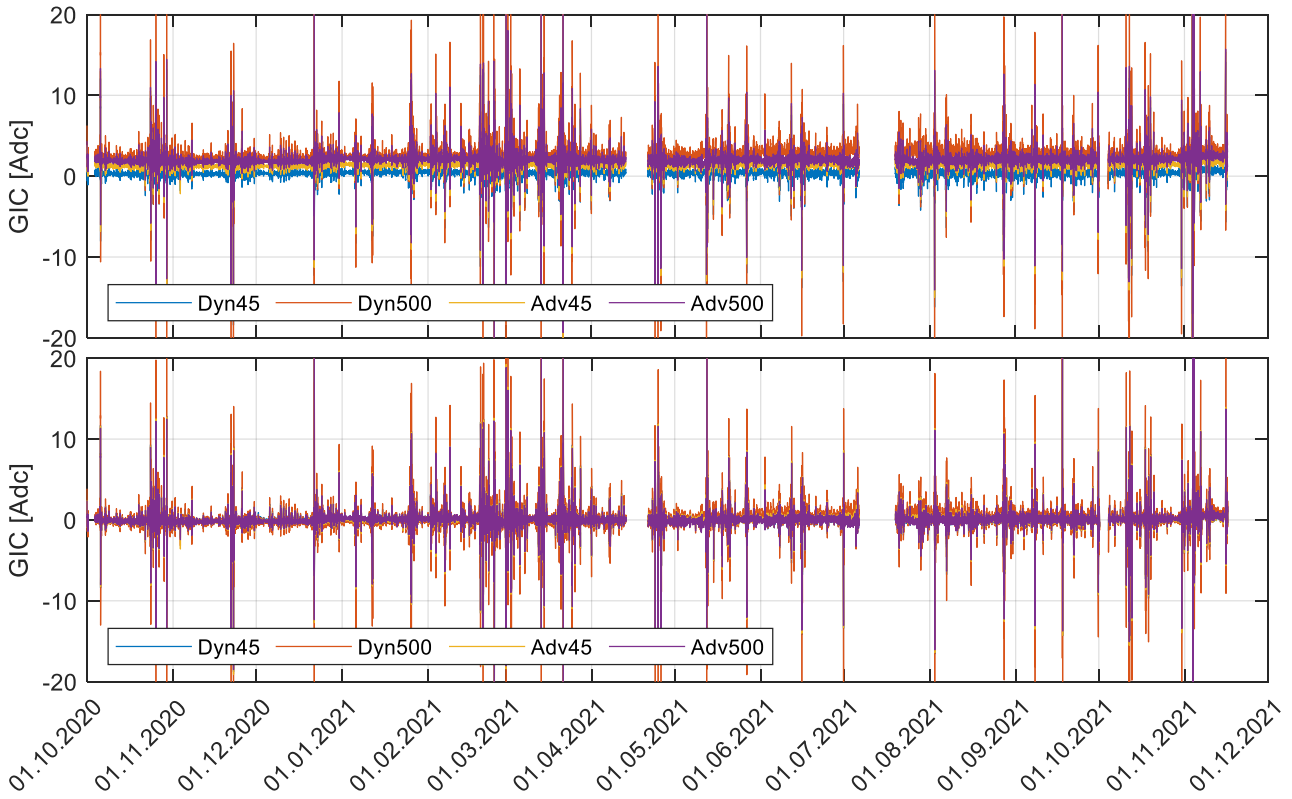


Figure 4-8: Measured GIC in 2020/2021 as recorded by data logger (upper) and offset-adjusted (lower).

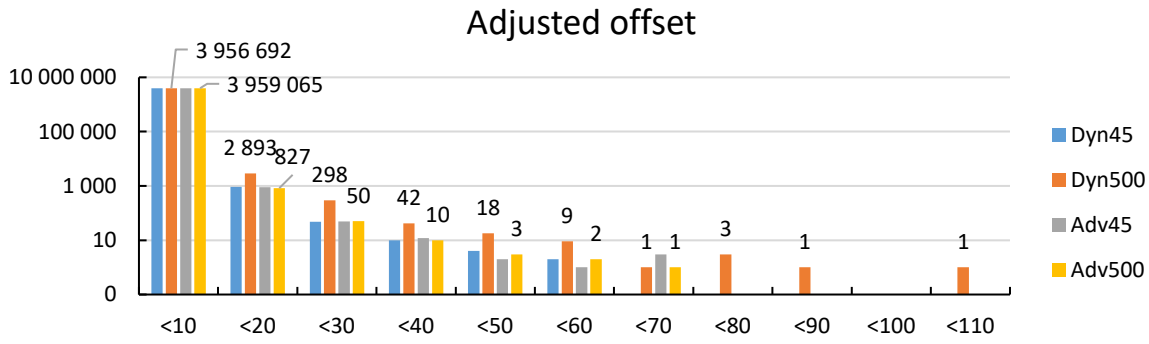


Figure 4-9: Number of measurements at different current with adjusted offset from GIC-sensors.

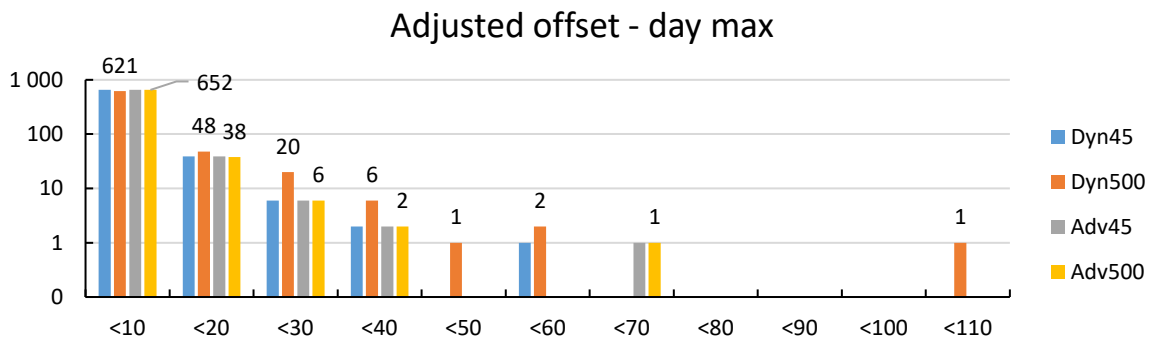


Figure 4-10: Number of measurements from data set where only maximum day value is given. The offset from GIC-sensors is adjusted.

5 RECORDING OF GEOMAGNETIC FIELDS

5.1 Introduction

A network of magnetometers, for local measurements of the Earth's magnetic field, are placed throughout Norway, with measurements dating back several decades for many stations. Data from these instruments are available from Tromsø Geophysical Observatory, a part of UiT – The Arctic University of Norway. In this report, the data from the magnetometer in Rørvik is used. The data are measured every 10 seconds. Two measurements are done every second, and it is the average that is saved.

There are three sources to the magnetic field that is measured by the magnetometers:

- the dynamo in the Earth's Crust (main contributor, normally about 90%),
- permanent magnetizing in the Earth's Crust (dependent on location), and
- external magnetic field that is the sum of currents in the ionosphere and secondary, induced currents in the ground (Earth's crust and the Earth's mantle). In events with very rapid changes in the magnetic field, the secondary ground currents can contribute to up to 40% of the total external field. Normally, the external field contributes less than 5 % of the total field. However, it is this component which contributes all the rapid variability in the measured field and, thus, constitutes the cause of GICs.

The variables below are included in the data set available from the Tromsø Geophysical Observatory. Only the two first are used in this report.

- Dec (declination) - Angular direction (°) of the horizontal component of the magnetic field. It is zero when the field is directed to north and has a positive direction when the field is eastwards.
- Horiz (horizontal) - horizontal component of the magnetic field [T] (B_{Horiz})
- Vert (vertical) - vertical component of the magnetic field [T]
- Incl (inclination) - angle of Vert [°]
- Total (absolute value of vector sum of Horiz and Vert) [T]

Between 16.01.2020 and 21.01.2020, the data were missing due to an instrument malfunction.

The following equations are used to modify the data set to get the variation in magnetic field. See conventions in the vector diagram, Figure 5-1. The number "10" is from the 10 second sampling interval of the geomagnetic field.

$$B_{North} = B_{Horiz} \cdot \cos(Dec) \quad \text{Eq. 5.1}$$

$$B_{East} = B_{Horiz} \cdot \sin(Dec) \quad \text{Eq. 5.2}$$

$$\frac{d}{dt} B_{North} = \frac{(B_{North}(t+1) - B_{North}(t))}{10} \quad \text{Eq. 5.3}$$

$$\frac{d}{dt} B_{East} = \frac{(B_{East}(t+1) - B_{East}(t))}{10} \quad \text{Eq. 5.4}$$

$$\left| \frac{dB}{dt} \right| = \sqrt{\left(\frac{d}{dt} B_{North} \right)^2 + \left(\frac{d}{dt} B_{East} \right)^2} \quad \text{Eq. 5.5}$$

$$\theta = \text{atan}_2\left(\frac{d}{dt} B_{\text{East}}, \frac{d}{dt} B_{\text{North}}\right) \quad \text{Eq. 5.6}$$

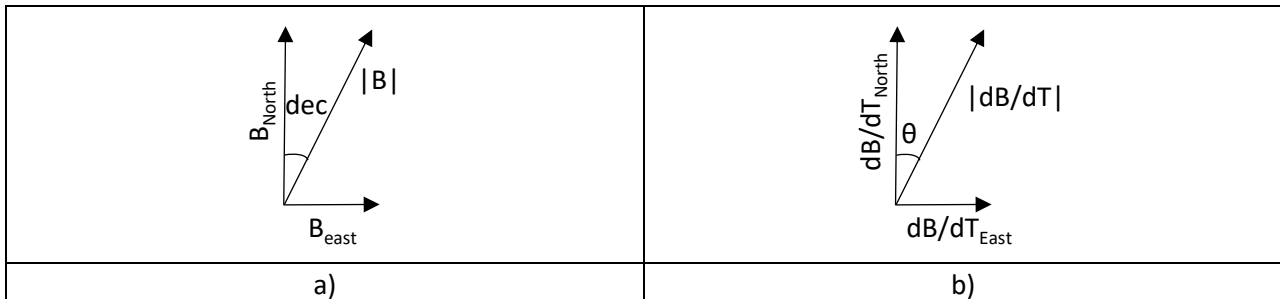


Figure 5-1: Vector diagram of the magnetic field (a) and derivative of magnetic field (b).

5.2 Recordings 2019-2021

5.2.1 Geomagnetic field

An overview of the geomagnetic field recordings from 2019/2020 and 2020/2021 are seen in Figure 5-2 and Figure 5-3, respectively. A comparison to measured GIC is given in Section 6. The number of high readings and amplitude seem at a first glance to correlate with GIC. As for GIC, there is more activity in 2020/2021 than the previous year. As can be seen, there is an offset in the geomagnetic field, around $1.3e4$ nT. This is due to the natural magnetic field around the Earth. The spikes represent mostly the external variation.

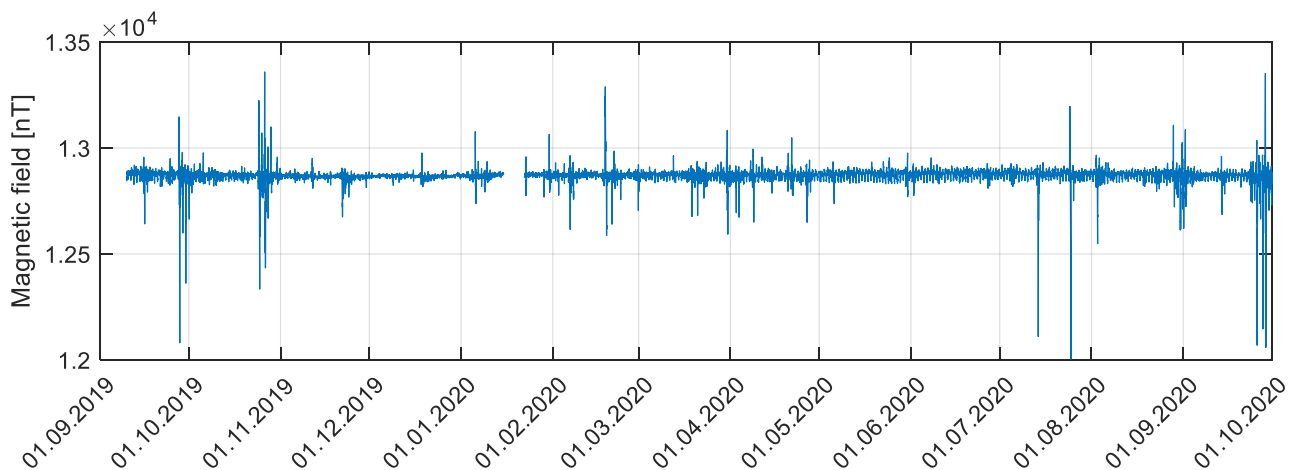


Figure 5-2: Horizontal component of the geomagnetic field in 2019/2020.

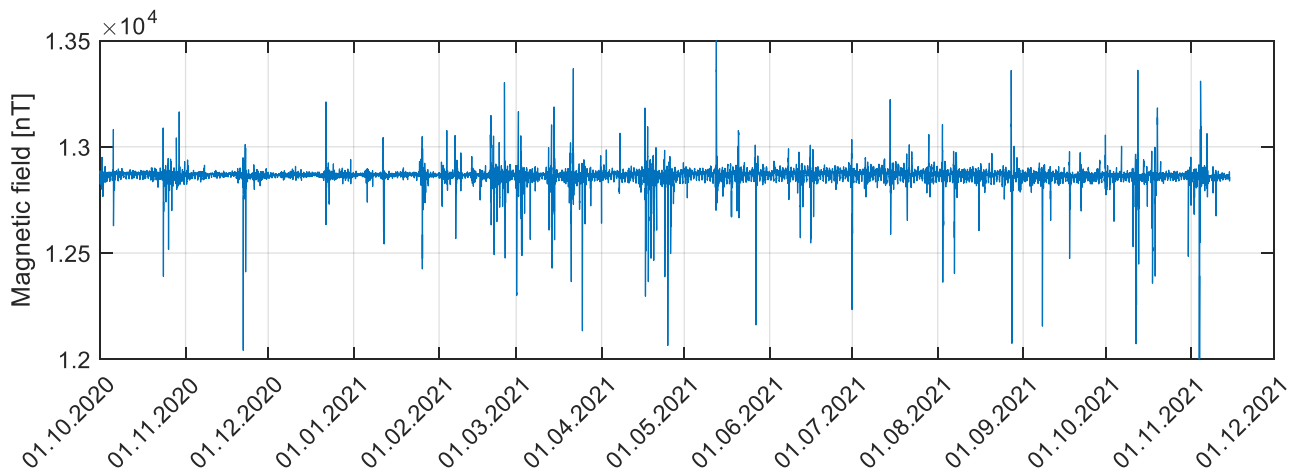


Figure 5-3: Horizontal component of the geomagnetic field 2020/2021.

In the two previous figures, the horizontal component is shown. Being almost parallel to true North, this becomes apparent when the horizontal component is decomposed into a North and East component. This is seen in Figure 5-4, where the north vs east components are plotted. The angle to north is between 2.9 and 7.0°, while the angle reference to the east component is between 83.0 and 87.1°.

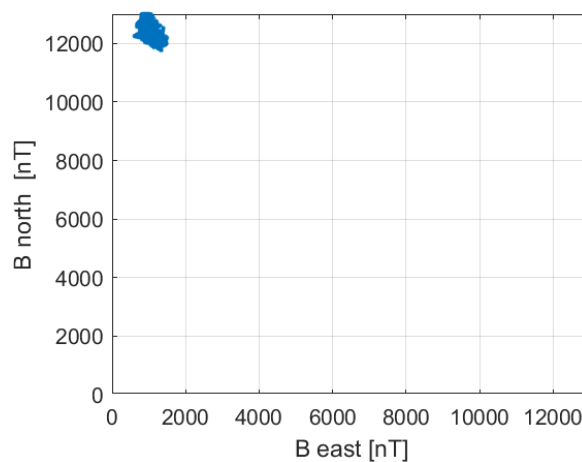


Figure 5-4: North and east component of geomagnetic field 2020/2021.

In the total geomagnetic field (sum of dynamo, crust and external field), the north component dominates in the horizontal plane, as the magnetic field is directed towards north. Therefore, the north component of the magnetic field is horizontal component the magnetic field (as seen in Figure 5-4). Since the internal and crustal fields have no influence on dB/dt on short time scale, it is more relevant to look at the magnetic field when these (i.e. median of data set) are removed. For the North component, the median is 12837 nT. For the East component, the median is 916.7 nT. The average values are 12834 and 917.8 nT, respectively. The plots are seen in Figure 5-5 (north component) and Figure 5-6 (east component). Note that for the east component, the incline around the y-axis is caused by the secular variation of the internal field during the two years. The electrojets (auroral oval) is approximately a circle around the geomagnetic pole, and therefore, the external field is mainly caused by an ionospheric current in the east-west direction. This means that the external field is dominated in the north- south-direction, as seen in Figure 5-7. The external geomagnetic field has a much larger variety in orientation than the total geomagnetic field.

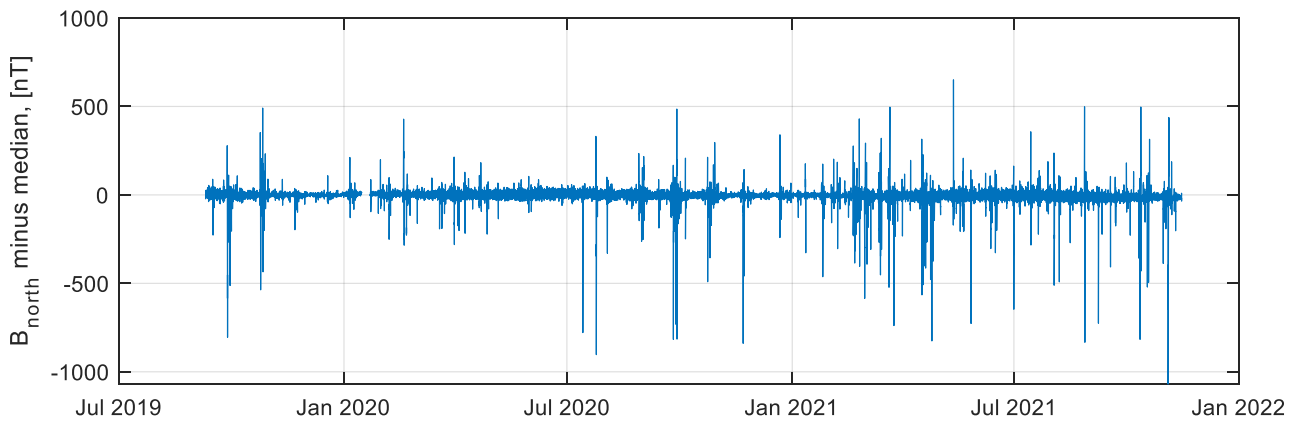


Figure 5-5: North component of the geomagnetic field minus its median (12837e4 nT).

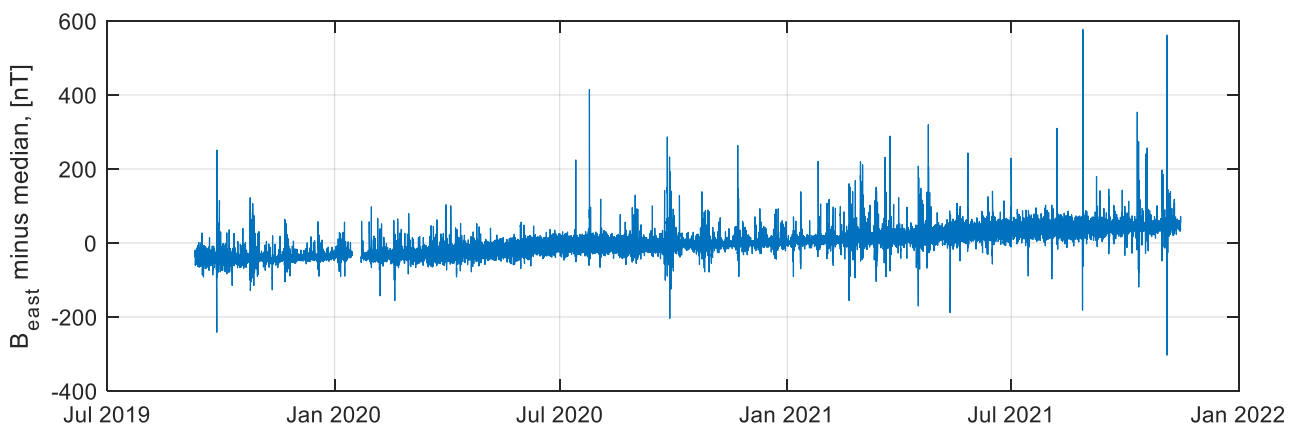


Figure 5-6: East component of the geomagnetic field minus its median (916.7 nT).

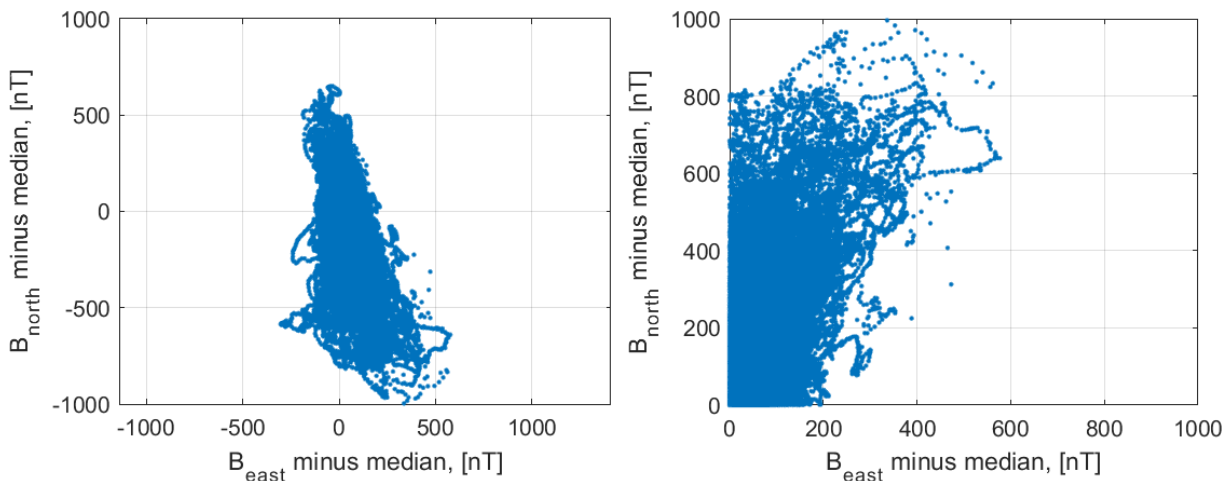


Figure 5-7: North and east component of geomagnetic field minus their medians 2020/2021. Right: absolute value of left figure.

5.2.2 Variation in magnetic field

The variation in the magnetic field (dB/dt), that will be compared to GIC, is seen in Figure 5-8 and Figure 5-9. The trend is similar as for the absolute value of the magnetic field. A difference is however the angle between the north and east component. For the magnetic field, the north component dominates.

However, for the dB/dt, the angle does not correlate for one specific angle, see Figure 5-10. This indicates that transmission lines with east-west orientation are as vulnerable to GIC as transmission lines oriented north-south. The trend is valid at the location of this specific transformer where GIC is measured and assumes that the electrical field is distributed similar as dB/dt. Local variations in the geological conditions can result in different conclusions at other locations.

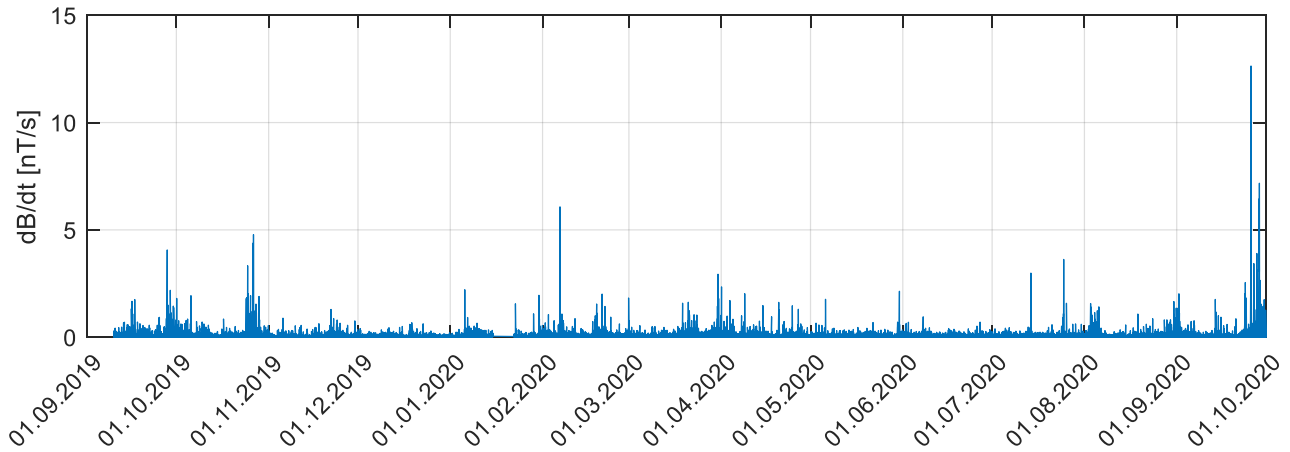


Figure 5-8: Recorded variation in geomagnetic field (dB/dt) in 2019/2020.

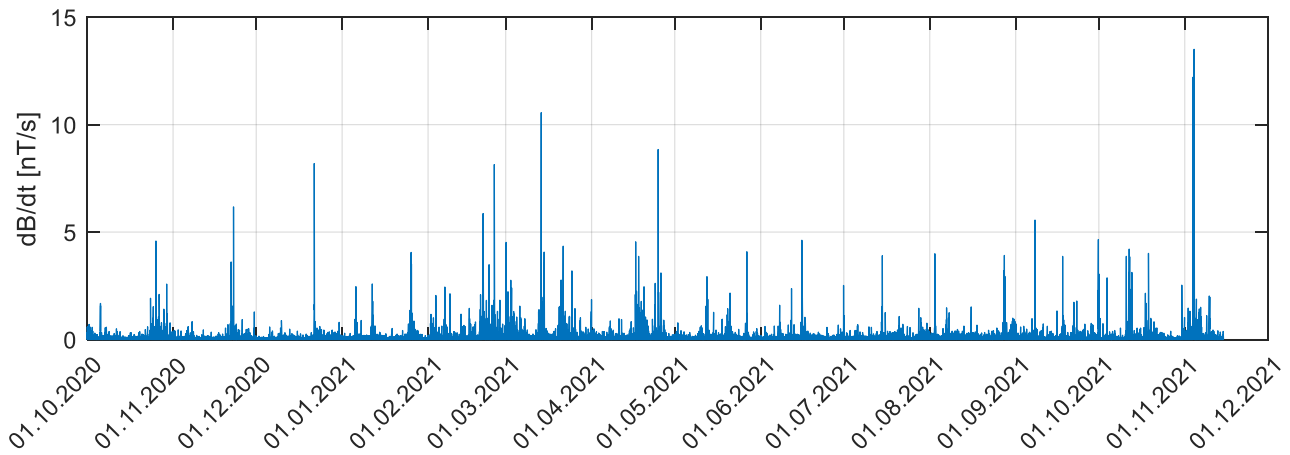


Figure 5-9: Recorded variation in geomagnetic field (dB/dt) in 2020/2021.

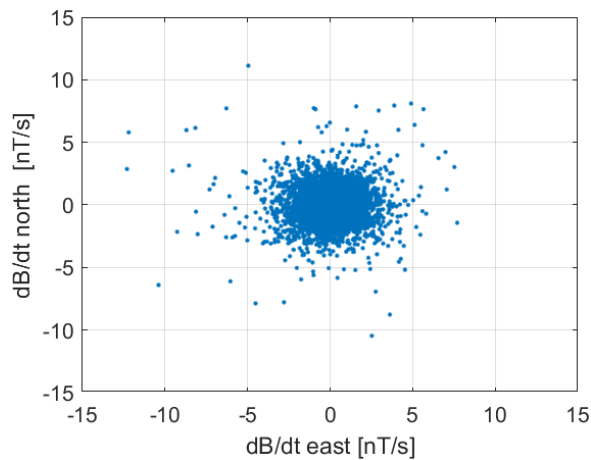


Figure 5-10: East and north component of variation in geomagnetic field (dB/dt).

6 COMPARISON BETWEEN GIC AND dB/dT

In this section, the recorded geomagnetic currents and variation in geomagnetic field are compared. It is important to note that the GIC-recordings are time instant every 15th second, while recording of the magnetic field is a 10 second average. The data from sensor Adv500 is used in this section, as this sensor has sufficient range (+/- 500 A) and the measurements are similar as the Dyn45 and Adv45 sensors. It is also chosen in preference to Dyn500, as this sensor showed higher readings than the other three.

6.1 Recordings 2019-2021

An overview of the recordings from 2019/2020 and 2020/2021 are given in Figure 6-1 and Figure 6-2. As can be seen, there is some correlation between GIC and dB/dt: each of the variables fluctuate at the same time instances. However, the magnitude has not the same clear correlation. This is further investigated in the next sections.

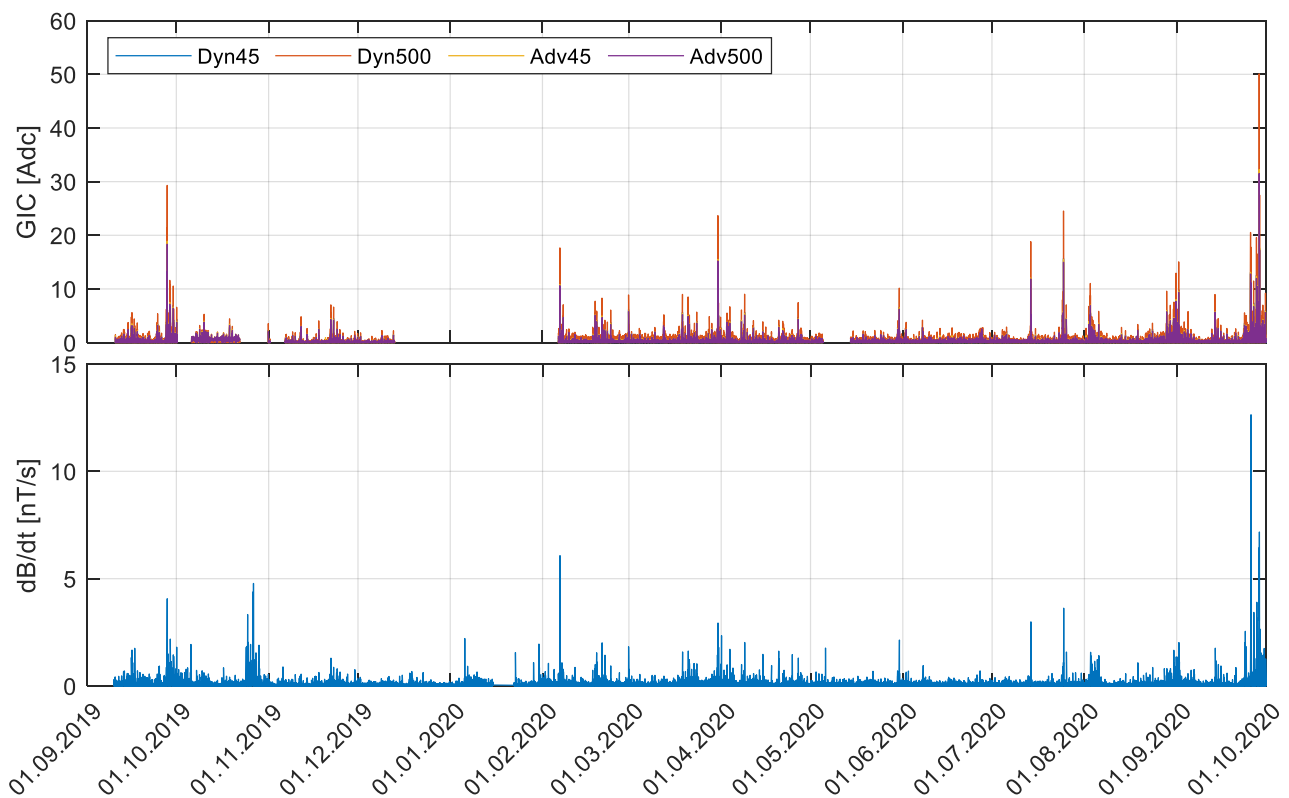


Figure 6-1: Geomagnetically induced current (GIC) and variation in the geomagnetic field (dB/dt) in 2019/2020. dB/dt is from the absolute value in the dataset.

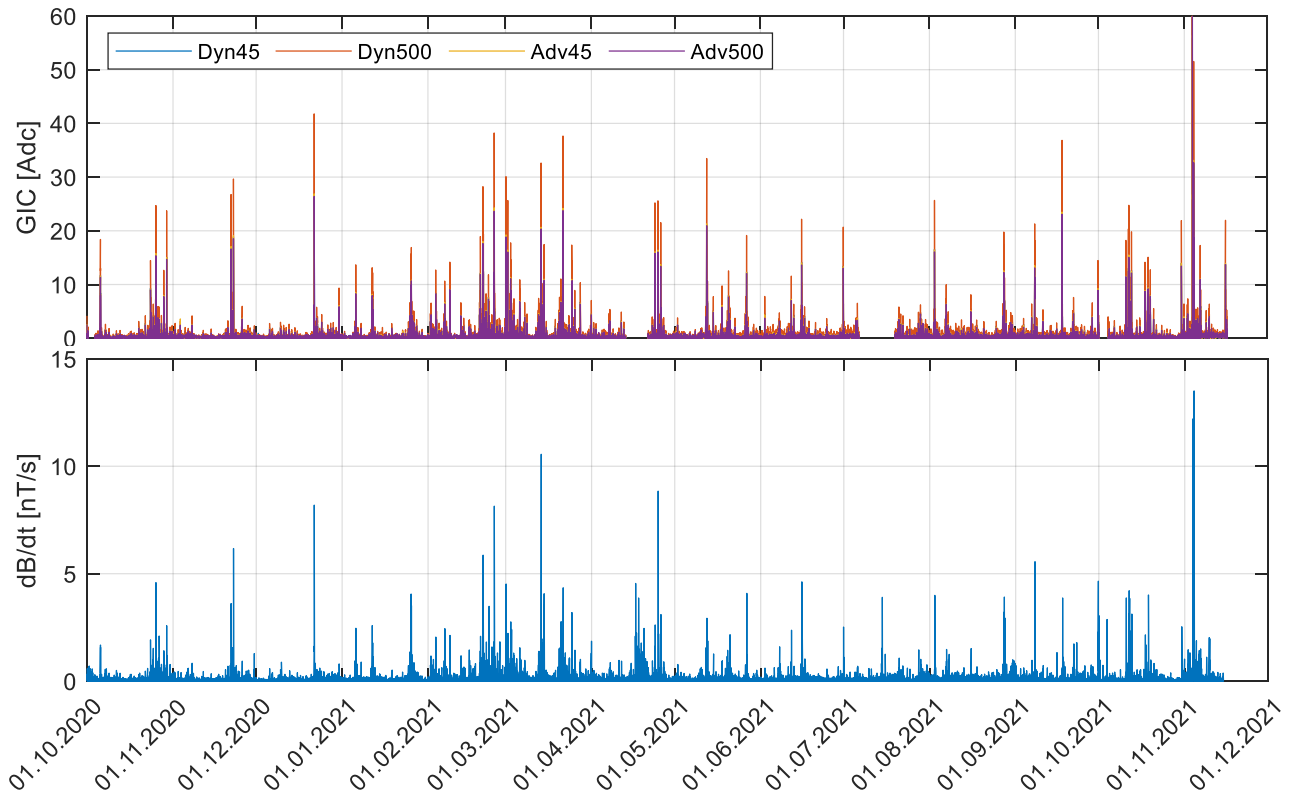


Figure 6-2: Geomagnetically induced current (GIC) and variation in the geomagnetic field (dB/dt) in 2020/2021. dB/dt is from the absolute value in the dataset.

6.2 Recordings 27.09.2019, 28.09.2020 and 03.11.2021

In this section, the three GIC incidents 27.09.2019, 28.09.2020 and 03.11.2021 are considered. The intention is to visualize the correlation in amplitude and shape between GIC and dB/dt. It is clear from all three instances that there is a correlation, but, as seen before, the correlation is not perfect. It is evident that GIC is present for variations in dB/dt, but correlation in amplitude varies. More prominent is that the shape differs. It is seen that the dB/dt varies more frequent than GIC. See Figure 6-3, Figure 6-4 and Figure 6-5.

Please note that there is some mismatch in the time stamps between GIC and dB/dt. The GIC time is up to a few minutes behind due to time inaccuracies in the computer that is connected to the data logger.

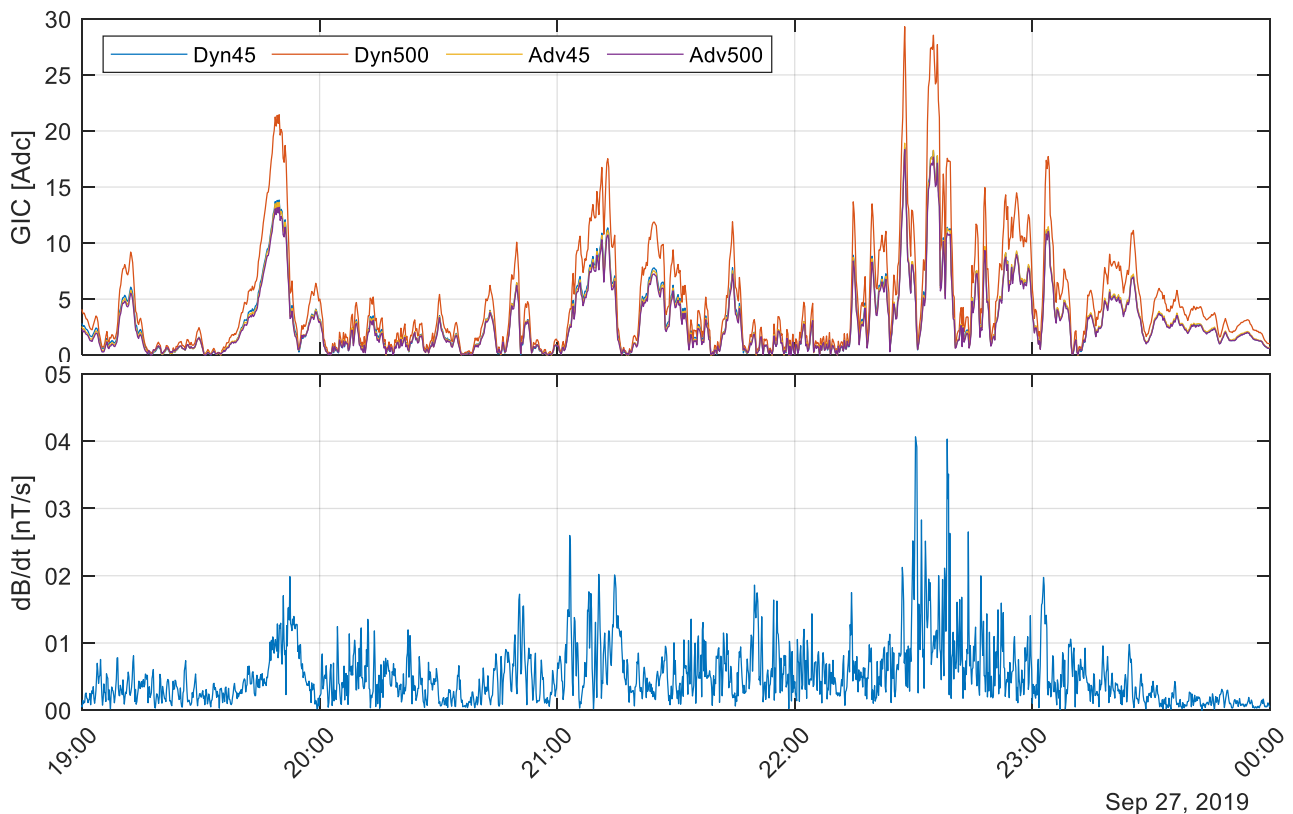


Figure 6-3: Variation in geomagnetic field and geomagnetically induced current 27. September 2019. Note that the GIC time is up to a few minutes behind of dB/dt time.

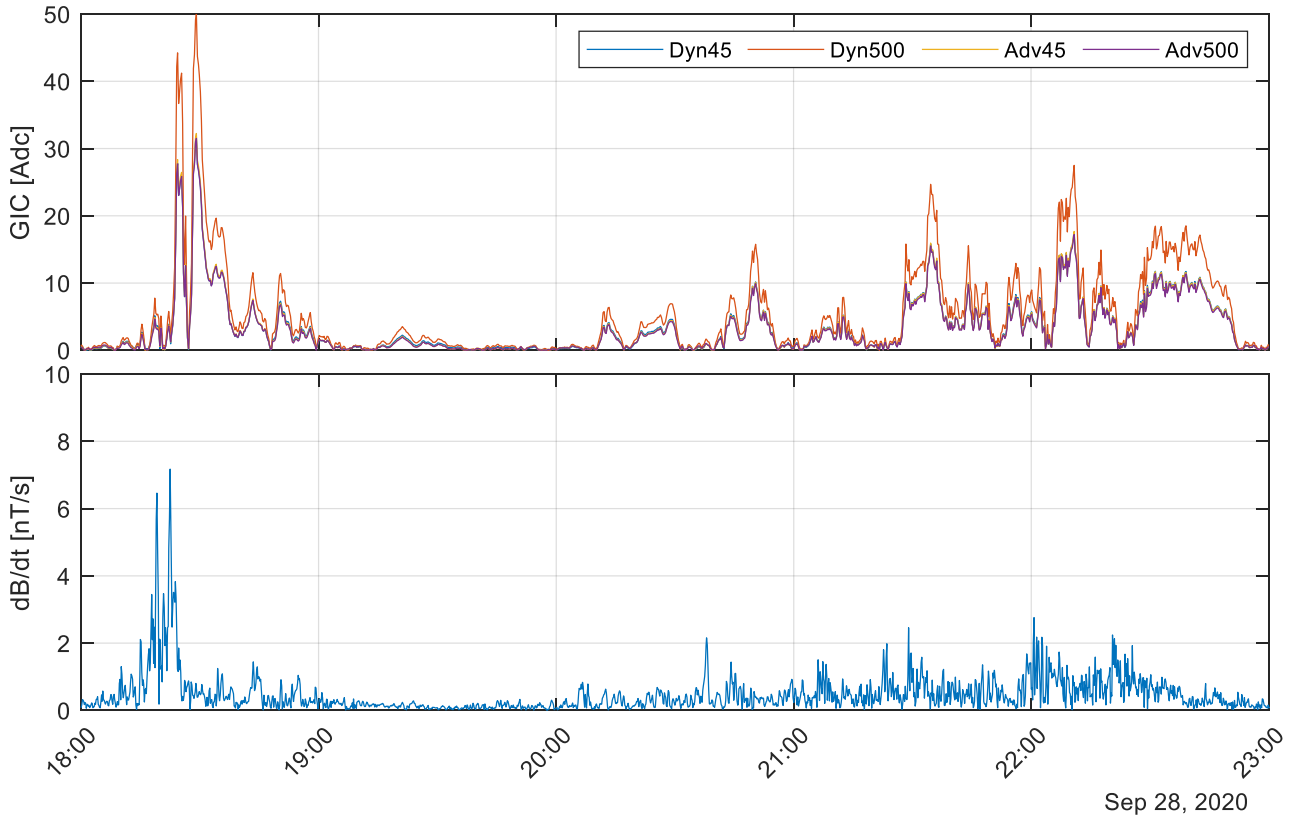


Figure 6-4: Geomagnetic field and geomagnetically induced current 28. September 2020. Note that the GIC time is up to a few minutes behind of dB/dt time.

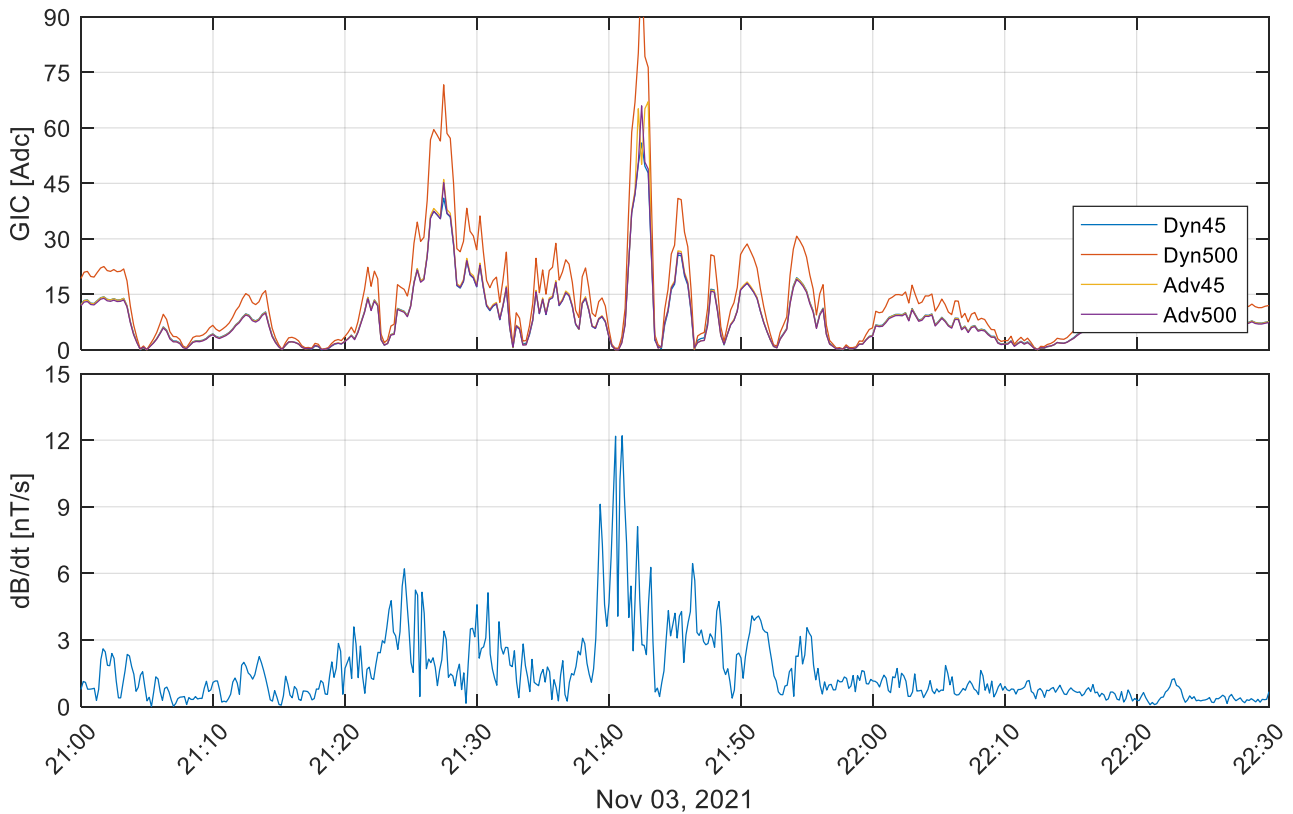


Figure 6-5: Variation in field and geomagnetically induced current 03.11.2021. Note that the GIC time is up to a few minutes behind of dB/dt time.

6.3 Correlation GIC and dB/dt

The correlation between GIC and dB/dt has been calculated based on linear regression. The dataset with maximum values for each day (699 data points) and from each hour (16 515 data points) are evaluated, see Figure 6-6. For perfect correlation between the data points, all dots would be on one line. There are more data points for lower GIC and dB/dt, but the result seems to be similar even if the lower readings are removed.

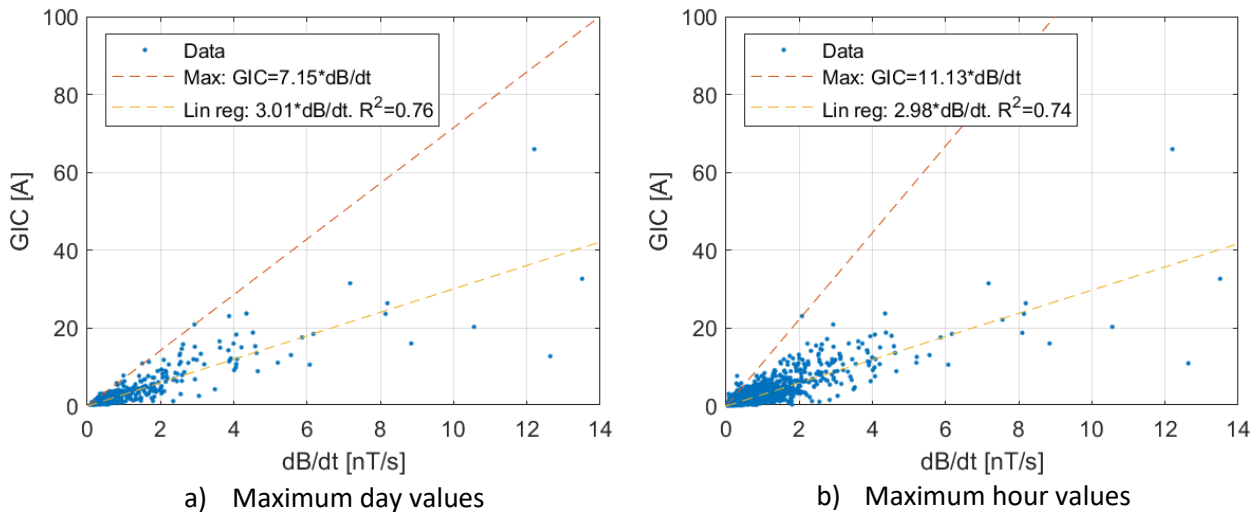


Figure 6-6: Variation in geomagnetic field vs geomagnetically induced current Orientation and magnitude of geomagnetic field as measured.

The regression, for hour-max and day-max dataset, shows that measured GIC (A) is about three times the measured dB/dt (nT/s), as indicated in the Eq. 6.1. The coefficient of determination (R^2), a statistical value that examines how differences in one variable can be explained by the difference in a second variable, is about 0.74-0.76. A perfect fit would give a coefficient of 1.

$$GIC [A] = 3 \cdot \frac{dB}{dt} \left[\frac{nT}{s} \right] \quad \text{Eq. 6.1}$$

From the plots, it seems to be a maximum GIC for each dB/dt, where GIC is always less than 7 times dB/dt. As there is mismatch in recorded time of GIC and dB/dt, the day-max values are considered more accurate than the hour-max values.

$$GIC [A] < 7 \cdot \frac{dB}{dt} \left[\frac{nT}{s} \right] \quad \text{Eq. 6.2}$$

A better correlation (R^2 closer to 1) may be found if looking at the magnetic field projected in the same angle as the transmission line connected to the transformer. Angles from 0° north to 90° north (meaning east) with interval of 15° is evaluated. The transmission lines to and from the transformer are installed at an angle of about 15° east of north.

The projection of B (magnetic field, called Horiz in Section 5.1) with an angle v_B (called Dec in Section 5.1) into the vector P with angle v_P , along the line p is given by the two equations below. P_E is the east component and P_N the north component of P . Similar as in Section 5.1, derivation is done on the north and east components (not on the scalar P). After derivation, the vector sum of the two components is used. The variables are indicated in Figure 6-7. In Figure 6-8, projection is visualized for a vector with length 10 and 10° . For a projection on 0° ref y-axis, the vector becomes 0 (x) and 9.85 (y). A projection on 90° ref y-axis, gives the vector 1.74 (x), 0 (y).

$$P = B \cdot \cos(v_P - v_B) \quad \text{Eq. 6.1}$$

$$P_N = P \cdot \sin(v_P) = B \cdot \cos(v_P - v_B) \cdot \cos(v_P) \quad \text{Eq. 6.2}$$

$$P_E = P \cdot \cos(v_P) = B \cdot \cos(v_P - v_B) \cdot \sin(v_P) \quad \text{Eq. 6.3}$$

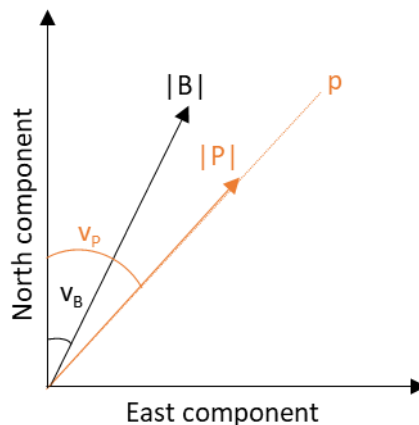


Figure 6-7: Geomagnetic field (peak) vs geomagnetically induced current with orientation as recorded.

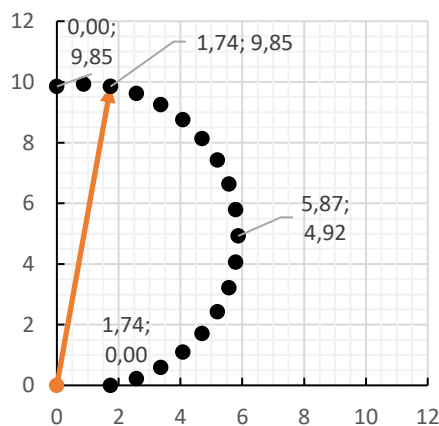
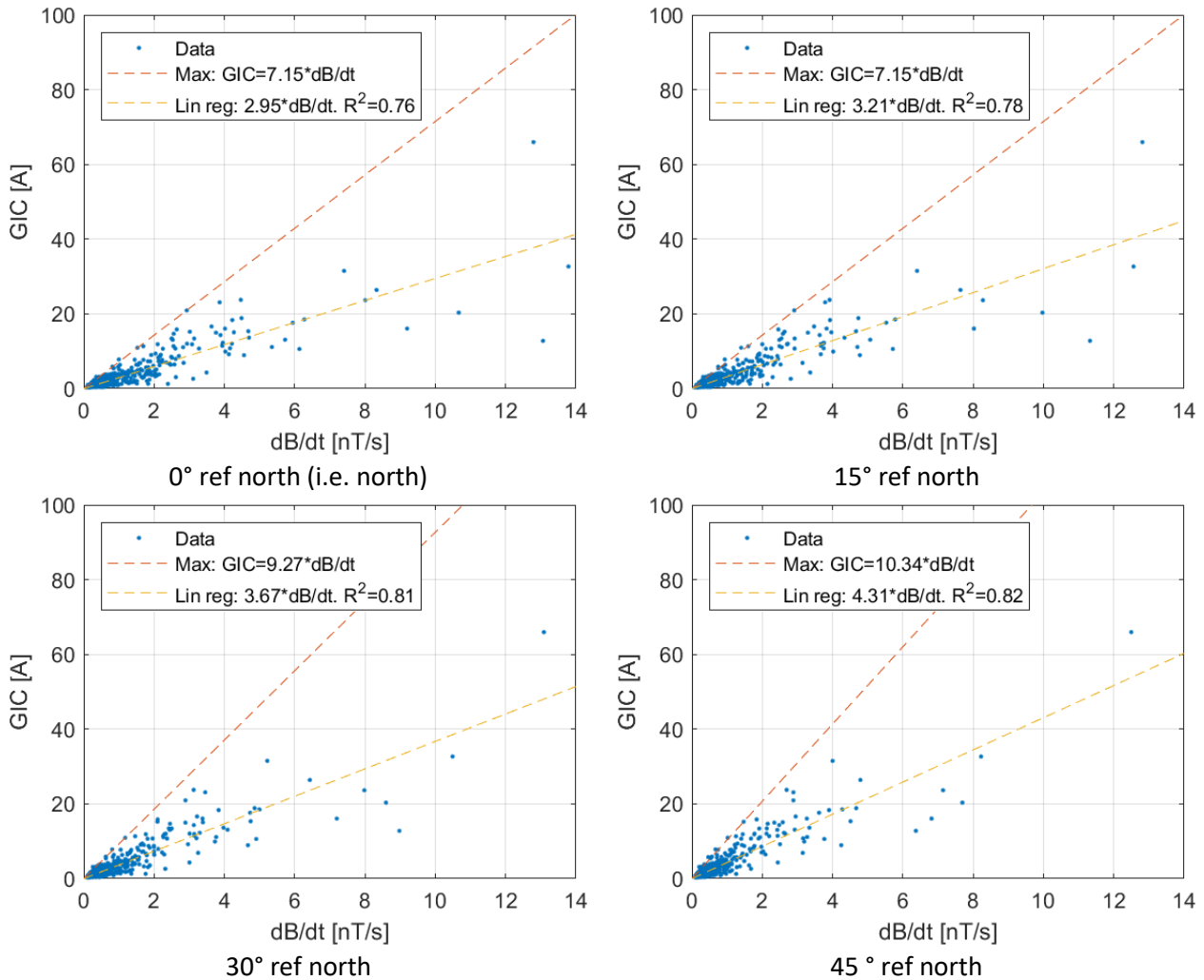


Figure 6-8: Visualization of projection for a vector with length 10 and angle 10° (ref y-axis) on a series of angles from 0 to 90° , with 5° intervals.

In Figure 6-9, the correlation between GIC and dB/dt are shown for projection of the measured geomagnetic field (originally 3-7° north if including the internal magnetic field, ref. Figure 5-4) to 0, 15, 30, 45, 60, 75 and 90° north (90° north is east). The transmission lines to and from the transformer are installed at an angle of about 15° north. Best correlation is seen for an angle of 45° (i.e. north-east), with highest coefficient of determination (R^2) of 0.82. Note that the linear regression gives a larger multiplication number between GIC and dB/dt. As, from Figure 5-10, dB/dt is not dominated in any direction, it is likely that the differences in Figure 6-9 is due to a non-uniform conductivity in the crust.



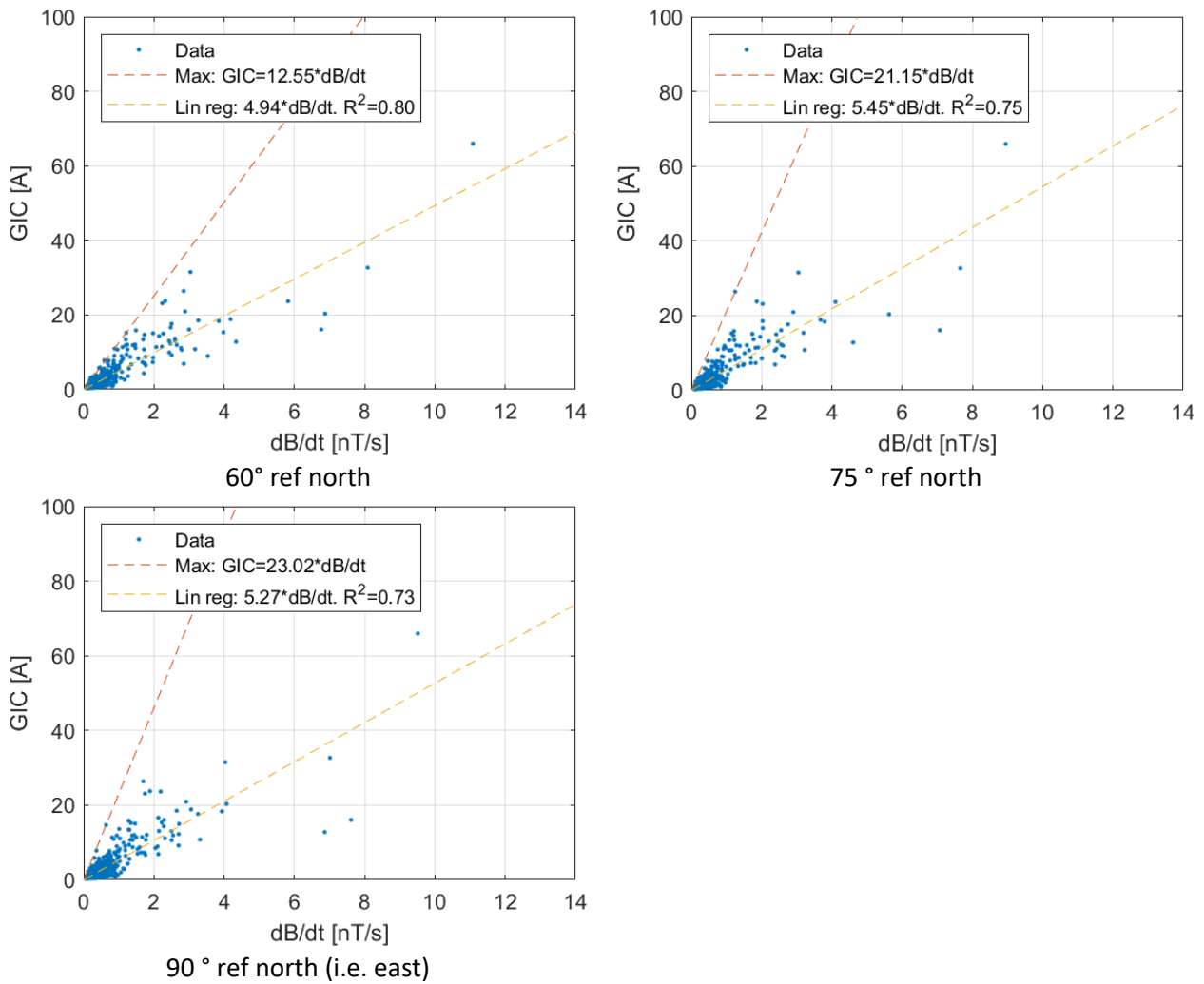


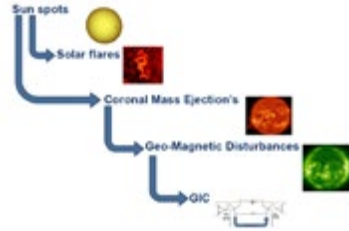
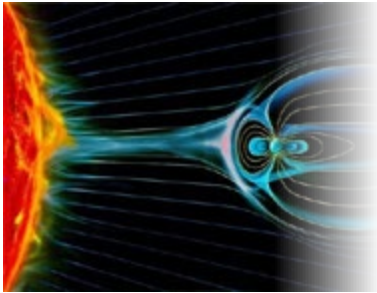
Figure 6-9: Variation in geomagnetic field (abs) vs geomagnetically induced current, with orientation between 0° north and 90° north. Dataset with day-maximum values is used.

7 REFERENCES

- [1] Olve Mo, Kristian Solheim Thinn, and SINTEF, "2021-00209 Tiltak for å håndtere risiko og motvirke konsekvenser knyttet til geomagnetisk induisert strøm i kraftnettet Rev. 2.0," ed, 2021.
- [2] H. Seljeseth and O. Rokseth, "Teknisk rapport 2958. Registrering av induserte strømmmer I kraftnettet P.G.A. partikkelstrøm fra sola.," SINTEF, Elektrisitetsforsyningens Forskningsinstitutt,, 1983.
- [3] J. D. Aspnes, R. P. Merritt, and B. D. Spell, "Instrumentation System to Measure Geomagnetically Induced Current Effects," *IEEE Transactions on Power Delivery*, vol. 2, no. 4, pp. 1031-1036, 1987, doi: 10.1109/TPWRD.1987.4308217.
- [4] L. Bolduc, "GIC observations and studies in the Hydro-Québec power system," *Journal of Atmospheric and Solar-Terrestrial Physics*, Article vol. 64, no. 16, pp. 1793-1802, 2002, doi: 10.1016/S1364-6826(02)00128-1.
- [5] T. Halbedl, H. Renner, M. Sakulin, and G. Achleitner, *Measurement and analysis of neutral point currents in a 400-kV-network*. 2014, pp. 65-68.
- [6] A. Viljanen, M. Myllys, and Finnish Meterological Institute, "Geomagnetically induced currents in the Norwegian high-voltage power grid: Statistics and extreme case estimations," ed, 2013.

APPENDIX A:

BROCHURES GIC-SENSORS



The substation hardened GIC-4 sensor is offered in fixed, split, and dual sensing cabinet packaging specifically designed for the measurement of Geomagnetic Induced Currents (GIC) in the transformer neutral ground connection. Split core models allow for rapid installation in energized applications.

Transformers at risk from GIC include:

- High voltage
- Grounded wye
- Autotransformers
- Y - Y
- Transformers interconnected with long transmission lines

GIC Sensors provide a means to sense, measure and communicate DC ground currents in harsh utility environments.

Features & Benefits

Ease of Installation

Fixed core sensors are ideal for new installations.

A large inner diameter (10.16 cm / 4 in. I.D.) conductor opening allows installation onto bus bars or round conductors.

The split core sensors allow the sensor to be installed on both new or existing transformer neutral ground connections without modification or the need to disconnect the ground. In most applications, the sensor can be installed while the transformer is energized.

A dual sensing cabinet model features a stainless steel enclosure and two installed sensors, allowing for rapid field installation.

Each sensor includes a type C conduit body and 1/2" NPT fitting for access to the conduit system for inspection, wire pulling and maintenance.

Sensors are constructed of a UV-resistant material for direct installation around a conductor without the need for a separate enclosure.

Ranges of Sensing

GIC Sensors are offered in three sensing ranges.

Model Range (Nominal)

Model	Range (Nominal)
L	+/- 45 Amps DC
H	+/- 360 Amps DC
5	+/- 500 Amps DC

Model L is designed for optimal resolution of small geomagnetic disturbances. Model H is designed for measurement of large coronal mass ejections, and Model 5 provides the industry's largest range of GIC sensing to include once in a hundred year events.

DC and Near DC Signals Only

The system has a built-in 4th order, low pass filter tuned to 3Hz. This ensures the output provides the desired signal with no interference from higher frequencies.

Noise Immunity

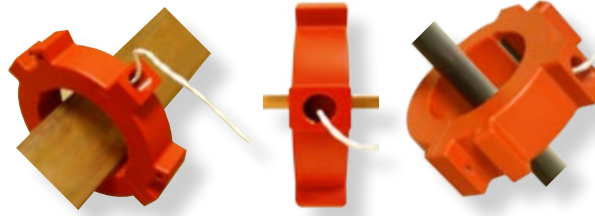
The sensor output is designed to provide maximum accuracy despite the high magnetic field environments that exist in the substation environment.

Temperature Stability

The selected sensor core ensures measurement accuracy of +/- 2% across the wide range of temperatures commonly found in a substation.

Applications

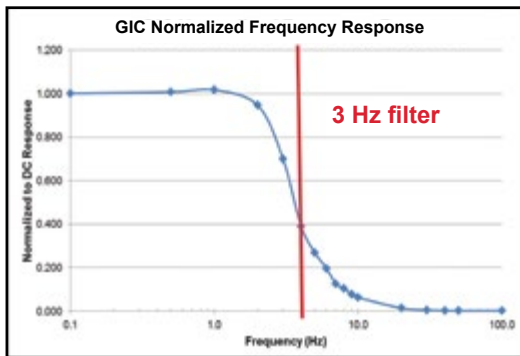
- **Copper Bus**
- **Bare Cable**
- **Insulated Conductors**



Designed to Detect GIC

The GIC-4 sensor is designed to outperform general purpose Hall Effect current transformers because it is specifically designed to measure a range of induced DC ground currents. Primary design differences are:

- **Exclusive detection of DC & Near DC Signals:** By properly monitoring geomagnetic induced currents GIC-4 includes both DC and near DC currents. Higher frequency currents (typically detected by standard Hall Effect current transducers) are filtered out.
- The GIC-4 sensor has a built-in filter tuned to 3Hz to block the higher frequency signals.
- The 4th order low pass filter, ensures the power frequency is effectively blocked, providing the desired output signal.

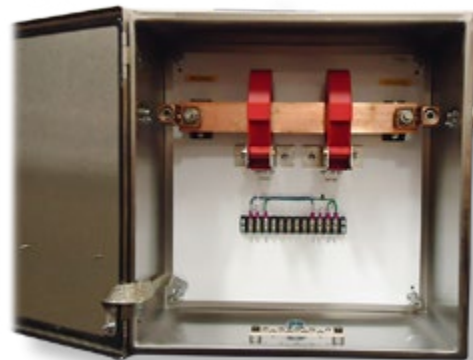


GIC Normalized Frequency Response

Single or Dual Range Sensing

Three models offer nominal sensing ranges of +/- 45A DC, +/- 360A DC, and +/- 500A DC.

Installing two sensors side-by-side with differing ranges provides the maximum precision and accuracy coverage of the majority of solar, coronal mass ejections (CME) where the lower range provides better resolution of smaller events and the higher range provides measurement for those once-in-a-hundred solar events.



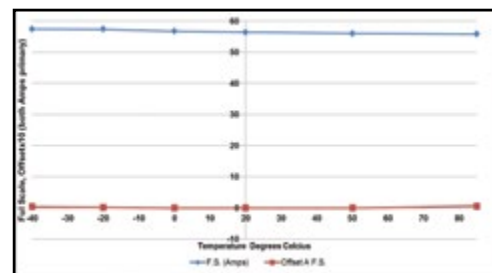
Dual GIC Sensing Cabinet

Accuracy is Temperature Stable

The core material selected for the sensor provides a consistently accurate reading across a wide range of operating temperatures.

The sensor measurement accuracy is proven to be:

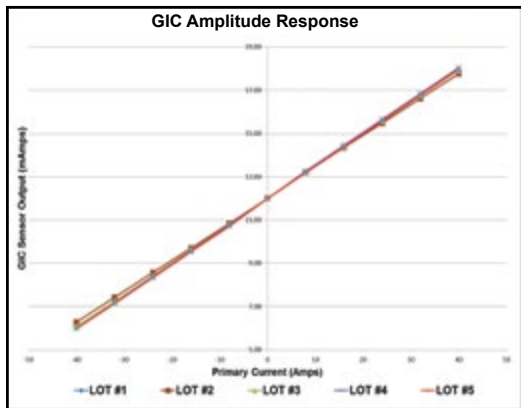
- +/- 1% accuracy: (0° C to 50° C / 32° F to 122° F)
- +/- 2% accuracy: (-40° C to 85° C / -40° F to 185° F)



Typical Characteristics vs. Temperature

Exceptional Linearity

The linearity of the GIC sensor output is exceptional. The GIC amplitude response graph illustrates sensor quality, linearity and consistency throughout the sensing range and over current and expanding production lots.



GIC Amplitude Response

Noise Resistant Output

The sensors 4-20mA output provides several advantages:

- Inherent voltage and four milliamperes of current are available to power the sensor and transmitter circuit. Sensor power and signal travel on one pair of wires.
- The current loop signal provides added noise immunity. The instrumentation will terminate the current loop utilizing a low ohm value resistor. Therefore, capacitive coupled noise does not have a significant effect on the desired output signal.
- The 4-20mA signal is unaffected by voltage drops, introduced by long connection wiring and associated terminations.
- There is positive indication of connection or sensor problems because instruments recognize a zero (0 mA) signal as an out of range value and will alert you of a problem.
- The signal is isolated. Differences in ground potential at the two ends of the loop do not affect the signal.
- The output is compatible with a wide number of instruments (4-20mA is a standard input for most instruments).

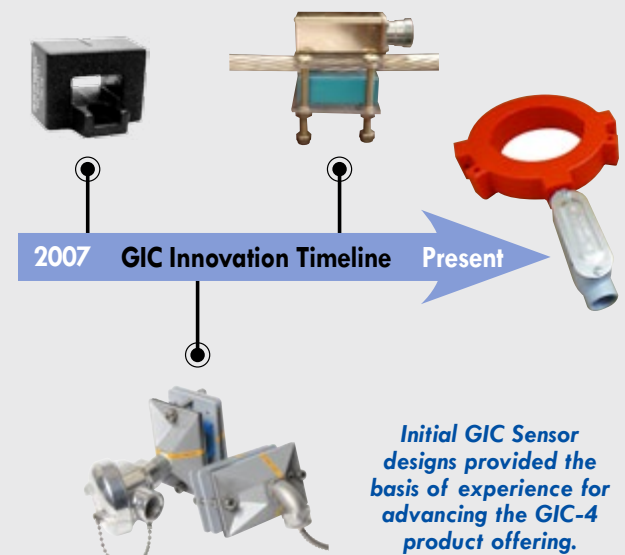
Building on Years of Experience

Dynamic Ratings installed the first Geomagnetic Induced Current (GIC) sensors in 2007. The first installations utilized a commercially available Hall Effect transducer. The sensor was installed in a separate enclosure and the transformer ground was modified to route through the enclosure.

In 2011 the number of customers interested in monitoring GIC expanded. Dynamic Ratings recognized the need to improve upon the basic, commercially available Hall Effect transducers available and invested in evaluating alternatives.

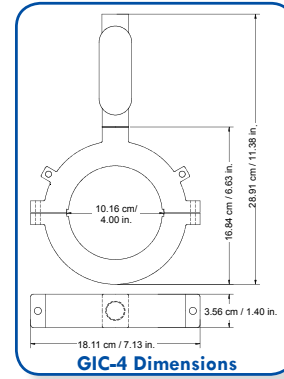
A substation hardened design concept was refined through rounds of product development innovation, resulting in fourth generation GIC sensors.

The GIC-4 sensor has proven to provide a dramatic improvement in performance and ease of installation.



SPECIFICATIONS

Sensing Range: <i>(Nominal)</i>	-45 to 45A DC -360 to 360A DC -500 to 500A DC
Output Signal:	Two wire; 4-20 mA
Power Source:	24V Loop Powered (12 to 36 V)
Accuracy:	+/- 1% at (0° C to 50° C / 32° F to 122° F) +/- 2% at (-40° C to 85° C / -40° F to 185° F)
Material Rating:	UV Resistant
Weight:	1.4 (kg) / 3.0 (lbs.)



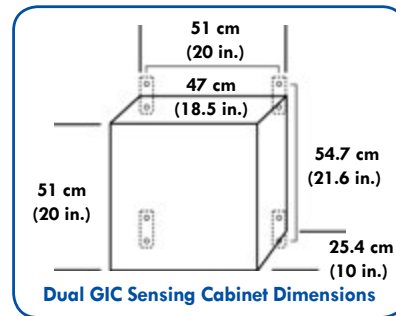
Note: A certificate of calibration provides the sensor's specific slope and offset.

Geomagnetic Induced Current (GIC) Sensors – Ordering Information

Part #	Sensing Range (Nominal)	Packaging	Description
GIC-4-F-L	-45 to 45 Amps DC	Fixed Core	One GIC Sensor with a 4th order low pass filter, including a type C, conduit body with 1/2" NPT type fitting.
GIC-4-F-H	-360 to 360 Amps DC	Fixed Core	
GIC-4-S-L	-45 to 45 Amps DC	Split Core	
GIC-4-S-H	-360 to 360 Amps DC	Split Core	
GIC-4-S-5	-500 to 500 Amps DC	Split Core	One GIC Sensor with a 4th order low pass filter, including a type C, conduit body with 1/2" NPT type fitting. This model includes factory installed core gap range adjustors.

Dual (GIC) Sensing Cabinets – Ordering Information

Part #	Sensing Range (Nominal)	Description
GICX2	-45 to 45 Amps DC and -360 to 360 Amps DC	Two GIC Sensors. Sensing range by part number is shown on the left. Each sensor has a 4th order low pass filter. Both sensors are packaged in a 51 cm x 51 cm x 25 cm / 20 in. x 20 in. x 10 in. Stainless Steel enclosure.



Asia / Africa / Oceania
+61 3 9574-7722
sales.asia@dynamicratings.com

Americas
+1 262 746-1230
sales.us@dynamicratings.com

Europe
+44 1617 681111
sales.eu@dynamicratings.com

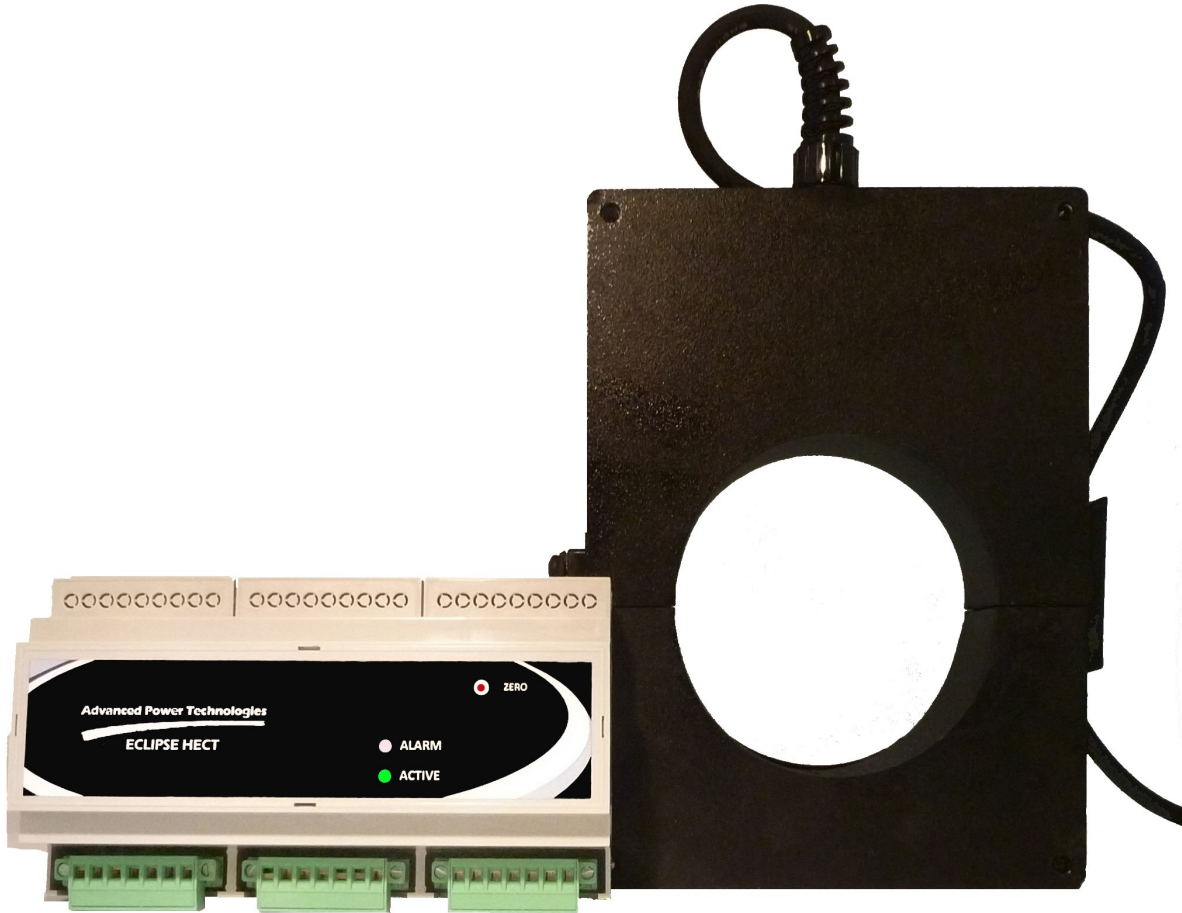
www.dynamicratings.com

Contact your sales representative for application assistance or pricing.

Advanced Power Technologies

ECLIPSE HECT ™

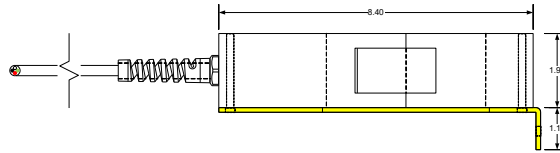
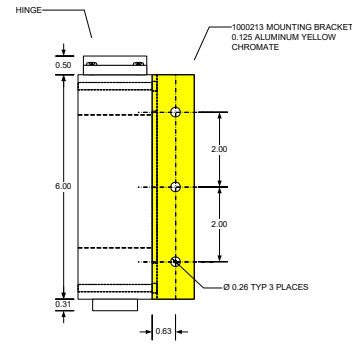
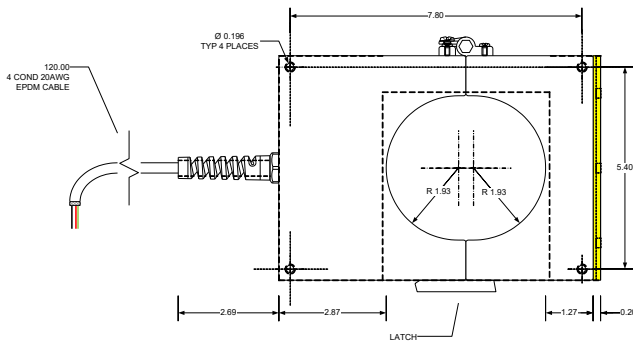
Monitor With Confidence™



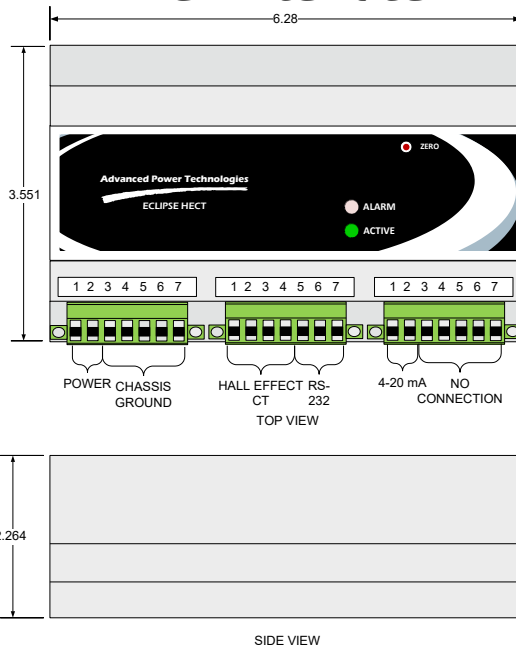
- ◆ For Monitoring GIC on Transformer Neutral
- ◆ Rugged Sealed Split Core Hall Effect CT for Outdoor use
- ◆ DIN Rail Mount Hall Effect CT Interface with 4-20 mA Analog Output



Split Core HECT ASSY with 1000123 Mtg Plate



HECT Interface



Ordering Part Numbers:

ECLIPSE HECT-001: Hall Effect Transducer Interface with Split Core CT

ECLIPSE HECT-002: Hall Effect Transducer Interface with Solid Core CT

1000213: Split Core Hall Effect CT Mounting Bracket

Spare Parts:

ECLIPSE HECT-000: Hall Effect Transducer Interface

57100200150: Split Core Hall Effect CT

Specifications

Power Supply Input Operating Range: 38 VDC to 290 VDC or 120 VAC +/- 10%, 2 Watts DC Max

Operating Temperature Range: -50 °C to +85 °C, 95% Relative Humidity (non condensing)

Analog Output: 4 to 20 mA. Maximum load 550 Ohms

Communications Interfaces: RS-232 3 Wire Interface (Rx, Tx, Ground)

Current Measurement Range: -500 to +500 Amps DC

Current Measurement Accuracy: +/- 2.8 % Full Scale


Current Measurement Resolution: 0.1 Amps DC

Attenuation: at 50 Hz & 60 Hz 80 dB maximum and 2nd harmonic above 60 dB minimum

Surge Withstand/Fast Transient: IEEE Std C37-90.1-2002.

Electrostatic Discharge: IEEE Std C37.90.3

Hall Effect CT IP Rating: IP65

EMC Directive (2004/108/EC): IEC61326-1 and CISPR-11 

www.AdvPowerTech.com

215 State Route 10, Building 2

Randolph, NJ 07869

Phone: (973) 328-3300

Fax: (973) 328-0666

APPENDIX B:

CALIBRATION CERTIFICATEs GIC-SENSORS

GIC Test Report

DR Job Number 8352

Style Option	Serial number	Date Tested	Tested By
Low Split Core	190426-02	4/26/2019	Curtis Cannon

Sensitivity mA/Amp	0.216
Slope Amp/mA (GICAARatio)	4.63
Full Scale Amps	37
Zero Line mA (GICRef)	11.98
Polarity	Forward
4mA = (Amps)	-36.9474
20mA = (Amps)	37.1326

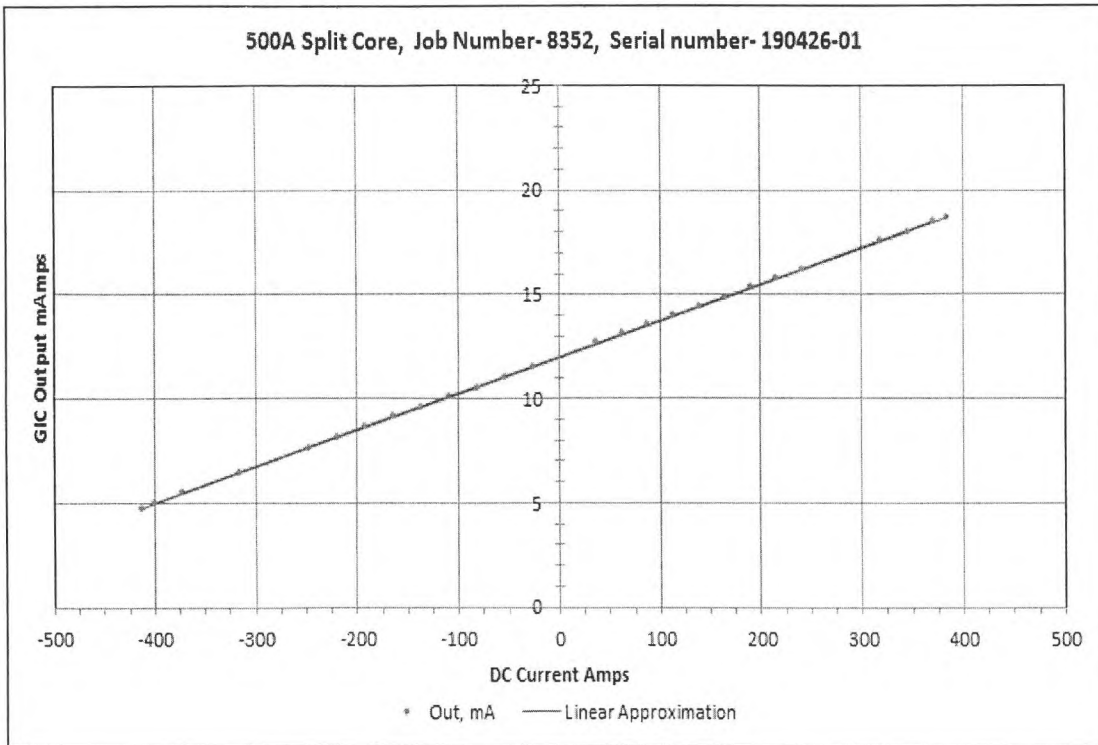


GIC Test Report

DR Job Number 8352

Style Option	Serial number	Date Tested	Tested By
500A Split Core	190426-01	4/26/2019	Curtis Cannon

Sensitivity mA/Amp	0.0175
Slope Amp/mA (GICARatio)	57.02
Full Scale Amps	456.2
Zero Line mA (GICRef)	12
Polarity	Forward
4mA = (Amps)	-456.16
20mA = (Amps)	456.16



Advanced Power Technologies

ECLIPSE HECT Interface Calibration Data Sheet
Rev C

M/N: <u>HBCF-000CB</u>	HECT S/N: <u>0200A</u>	Date: <u>6/11/2019</u>
	SENSOR S/N: <u>N/A</u>	
ECLIPSE HECT Firmware Version: <u>20180222</u>		
Customer: <u>SINTEF</u>		
Calibration (4-20mA):		
4.000 mAdc:	<input checked="" type="checkbox"/> Set	<input checked="" type="checkbox"/> Verified
20.000 mAdc: (may need a minute to come to equilibrium)	<input checked="" type="checkbox"/> Set	<input checked="" type="checkbox"/> Verified
Custom Input Range (default is 500Adc):		<input checked="" type="checkbox"/> Set <u>45</u> Adc
Calibration (Interface/Sensor):		<input checked="" type="checkbox"/> Interface-Only <u>N/A</u> <input type="checkbox"/> Interface+Sensor
+/-Cal Target Pt:	<u>45.00</u> Adc	<input checked="" type="checkbox"/> Set
+Target Pt Reading: <u>20.038</u> mAdc	<u>45.21</u> Adc	<input checked="" type="checkbox"/> Set
-Target Pt Reading: <u>3.970</u> mAdc	<u>45.17</u> Adc	<input checked="" type="checkbox"/> Set
Calibration Test (Interface/Sensor):		
Use this formula to calculate Adc from mAdc: (Reading mA - 12mA) / 8mA * Input Range		
+Target Pt Reading: <u>20.005</u> mAdc	<u>45.02</u> Adc	<input checked="" type="checkbox"/> Pass <input type="checkbox"/> Fail
-Target Pt Reading: <u>4.003</u> mAdc	<u>44.98</u> Adc	<input checked="" type="checkbox"/> Pass <input type="checkbox"/> Fail
ZERO (zero-cheater or sensor with no input):		<input checked="" type="checkbox"/> ZERO'ed
Print Status Screen:		<input checked="" type="checkbox"/> Printed
Comments:		
Tester: <u>D</u>	Approved: <u>SR</u>	

HECT SN0200A.TXT CAL @45A.TXT

STATUS

RAW HE LOAD=-0.03 AMP

HE LOAD=-0.04 AMP

HE ZERO OFFSET=-0.02 AMP

HE AUTO-ZERO OFFSET=0.00 AMP

CAL HE LOAD=-0.04 AMP

HE AUTO-ZERO AVERAGE=0.00 AMP

HE AUTO-ZERO SAMPLES=0

HE AUTO-ZERO ELAPSED PERIOD=0 MIN

CAL (+/-)TARGET=45.00 AMP

CAL OUTPUT @ (+)TARGET=45.21 AMP

CAL OUTPUT @ (-)TARGET=45.17 AMP

CAL SLOPE=0.9958 AMP/AMP

CAL Y-INT=-0.02 AMP

CAL DAC20=63008

CAL DAC4=12624

CAL DAC SLOPE=559.82

CAL DAC Y-INT=37816

PRESS ENTER TO GO BACK TO MAIN MENU

0200A

Advanced Power Technologies

Shipment Packing List

Shipment #: 246
S/O #: 14308

Customer #: SINTEF
Customer P/O #:

Order Date: 06 Jun 2019
Sched. Date: 19 Jun 2019


Ship Via: UPS Ground-UPS Ground

Bill To: SINTEF Energi AS
Sem Saelands vei 11
Trondheim 7034
Norway


Ship To: SINTEF Energi AS
Sem Saelands vei 11
Trondheim 7034
Norway

Attention: Kristian Thinn Solheim

Terms: Warranty


Order Line	Item Number Item Description	UOM	Ordered	Shipped	Verified	Status
001	ECLIPSE HECT-000CE Hall Effect Transducer Interface (CE) Hall Effect Transducer Interface CE	EACH	1.00	1.00		○

Notes: Replacement unit for ECLIPSE HECT (s/n: 0199A).
0199A shipped without the (+/- 45A) calibration

002	HECT CALIBRATION Eclipse HECT Interface Calibration (-45 to +45A)	EACH	1.00	1.00		○
-----	---	------	------	------	---	---



Notes: Provide copy of the calibration data sheet to the customer

Completed By: 

Checked By: 

ECLIPSE HECT Interface Test Data Sheet, Rev C

M/N: <i>HECT-001C3</i>	S/N: <i>0198A</i>	Date: <i>5/13/2019</i>
Customer: <i>SINTEF</i>		
Firmware Version : <i>20180222</i>		
48 Hour Burn-In Test and Power Supply - Record 5V Power Supply Output		
Burn-in :	<input checked="" type="checkbox"/> Pass	<input type="checkbox"/> Fail
38V DC In vs 5V Out (5.000V +/- 0.050V):	5V: <i>5.006V</i>	<input type="checkbox"/> Fail
290V DC In vs 5V Out (5.000V +/- 0.050V):	5V: <i>5.006V</i>	<input type="checkbox"/> Fail
120V AC In vs 5V Out (5.000V +/- 0.050V):	5V: <i>5.006V</i>	<input type="checkbox"/> Fail
RS-232 Communications		
RS-232 Communications & Programming:	<input checked="" type="checkbox"/> Pass	<input type="checkbox"/> Fail
RS-232 Firmware Patching:	<input checked="" type="checkbox"/> Pass	<input type="checkbox"/> Fail
Front Panel:		
ALARM LED:	<input checked="" type="checkbox"/> Pass	<input type="checkbox"/> Fail
ACTIVE LED:	<input checked="" type="checkbox"/> Pass	<input type="checkbox"/> Fail
ZERO BUTTON:	<input checked="" type="checkbox"/> Pass	<input type="checkbox"/> Fail
ECLIPSE HECT-000: HECT Input w/o GIC Sensor vs Analog Output (mA)		
Record Analog Output Reading		
4.000Vin across TB2-2&4 and 1.000Vin across TB2-3&4 (In vs. Out ≤ 1%) ¹	AOUT: <i>17.993mA</i>	<input type="checkbox"/> Fail
4.000Vin across TB2-3&4 and 1.000Vin across TB2-2&4 (In vs. Out ≤ 1%) ¹	AOUT: <i>6.015mA</i>	<input type="checkbox"/> Fail
NOTES: 1. AOUT reading should be: 12.000mA + 8mA * Vin / 4.000V		
ECLIPSE HECT-001/-002: HECT Input w/ GIC Sensor vs Analog Output (mA)		
Record Analog Output Reading ¹ , If Not ECLIPSE HECT-001/-002, Write N/A		
15A ² through GIC Sensor (Input vs. Output ≤ 5%) ³	AOUT: <i>12.222mA</i>	<input type="checkbox"/> Fail
-15A ² through GIC Sensor (Input vs. Output ≤ 5%) ³	AOUT: <i>11.760mA</i>	<input type="checkbox"/> Fail
30A ² through GIC Sensor (Input vs. Output ≤ 3%) ³	AOUT: <i>12.462mA</i>	<input type="checkbox"/> Fail
-30A ² through GIC Sensor (Input vs. Output ≤ 3%) ³	AOUT: <i>11.502mA</i>	<input type="checkbox"/> Fail
NOTES: 1. First ZERO with GIC Sensor connected and no current going through GIC Sensor. 2. 10 turns x 1.500A for 15A and 10 turns x 3.000A for 30A 3. AOUT reading should be: 12.000mA + 8mA * AmpsThroughGICSensor / 500A		

ECLIPSE HECT-001/-002: Failure Detection		
Positive Signal wire (Green) Failure Detection	<input checked="" type="checkbox"/> Pass	<input type="checkbox"/> Fail
Negative Signal Wire (Black) Failure Detection	<input checked="" type="checkbox"/> Pass	<input type="checkbox"/> Fail
Ground Wire (Black) Failure Detection	<input checked="" type="checkbox"/> Pass	<input type="checkbox"/> Fail
Terminal Block Failure Detection	<input checked="" type="checkbox"/> Pass	<input type="checkbox"/> Fail
COMMENT :		
TESTER : 		
APPROVED : 		

APPENDIX C:

DOCUMENTATION OTHER EQUIPMENT

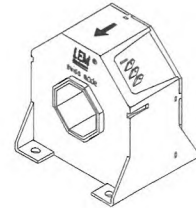
Current Transducer LT 1005-S

$$I_{PN} = 1000 \text{ A}$$

For the electronic measurement of currents : DC, AC, pulsed..., with a galvanic isolation between the primary circuit (high power) and the secondary circuit (electronic circuit).



0623



Electrical data

I_{PN}	Primary nominal r.m.s. current	1000	A					
I_P	Primary current, measuring range	0 .. ± 2000	A					
R_M	Measuring resistance @	$T_A = 70^\circ\text{C}$		$T_A = 85^\circ\text{C}$				
		$R_{M \min}$	$R_{M \max}$	$R_{M \min}$	$R_{M \max}$			
		with $\pm 15 \text{ V}$	@ $\pm 1000 \text{ A}_{\max}$	0	22.5	0	18.5	Ω
			@ $\pm 1200 \text{ A}_{\max}$	0	11	0	8	Ω
		with $\pm 24 \text{ V}$	@ $\pm 1000 \text{ A}_{\max}$	0	65	0	62	Ω
			@ $\pm 2000 \text{ A}_{\max}$	0	10	0	7	Ω
I_{SN}	Secondary nominal r.m.s. current	200	mA					
K_N	Conversion ratio	1 : 5000						
V_C	Supply voltage ($\pm 5 \%$)	$\pm 15 \dots 24$	V					
I_C	Current consumption	$30 (@ \pm 24 \text{ V}) + I_S$	mA					
V_d	R.m.s. voltage for AC isolation test, 50 Hz, 1 mn	6	kV					
V_b	R.m.s. rated voltage ¹⁾ , safe separation	1750	V					
		basic isolation	3500	V				

Features

- Closed loop (compensated) current transducer using the Hall effect
- Isolated plastic case recognized according to UL 94-V0.

Advantages

- Excellent accuracy
- Very good linearity
- Low temperature drift
- Optimized response time
- Wide frequency bandwidth
- No insertion losses
- High immunity to external interference
- Current overload capability.

Accuracy - Dynamic performance data

X_G	Overall accuracy @ I_{PN} , $T_A = 25^\circ\text{C}$	± 0.4	%	
ϵ_L	Linearity	< 0.1	%	
I_O	Offset current @ $I_P = 0$, $T_A = 25^\circ\text{C}$	Typ	Max	
			± 0.4	mA
I_{OT}	Thermal drift of I_O	$-10^\circ\text{C} \dots +85^\circ\text{C}$	± 0.3 ± 0.5	mA
t_r	Response time ²⁾ @ 90 % of I_{PN}	< 1	μs	
di/dt	di/dt accurately followed	> 50	A/ μs	
f	Frequency bandwidth (-1 dB)	DC .. 150	kHz	

Applications

- AC variable speed drives and servo motor drives
- Static converters for DC motor drives
- Battery supplied applications
- Uninterruptible Power Supplies (UPS)
- Switched Mode Power Supplies (SMPS)
- Power supplies for welding applications.

General data

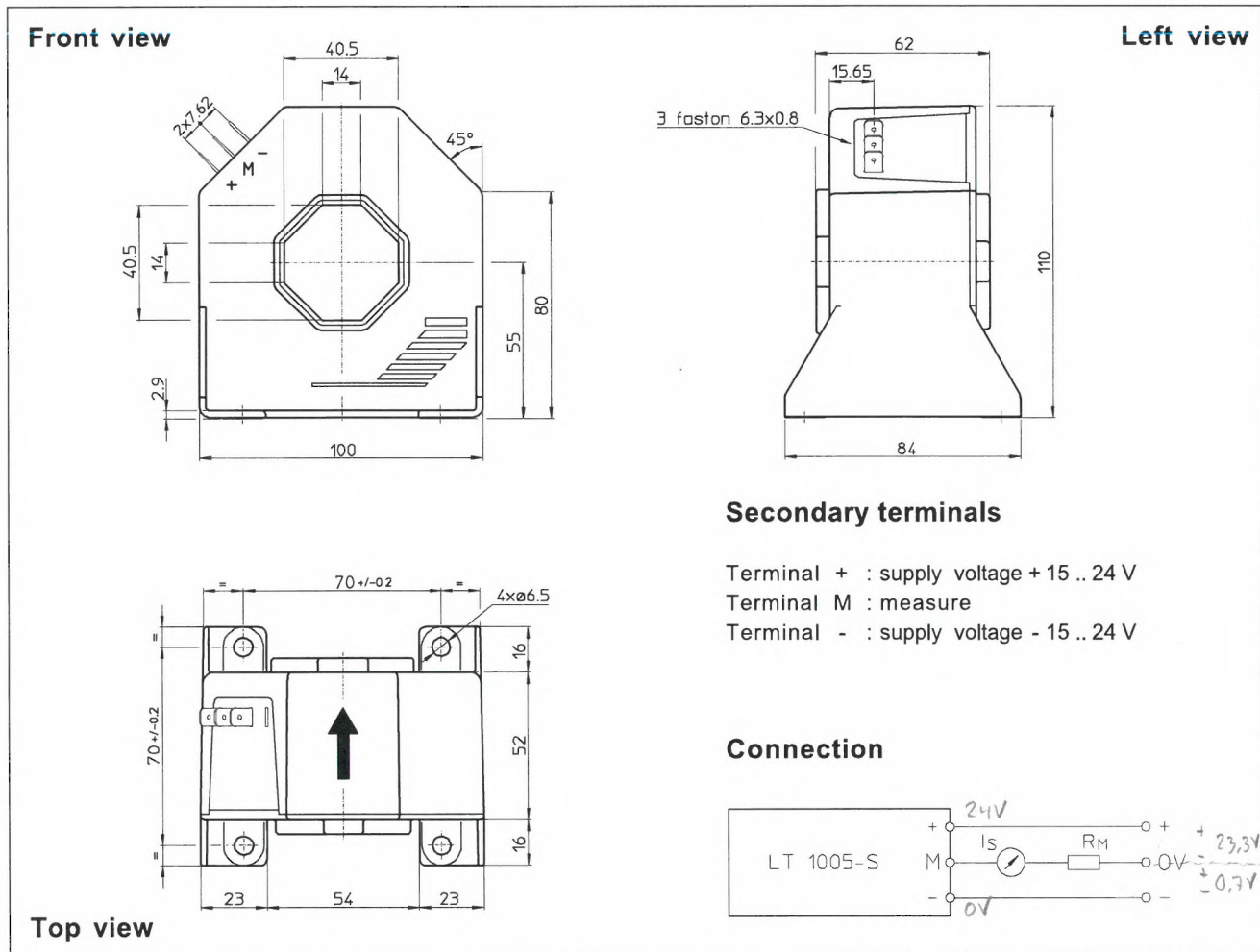
T_A	Ambient operating temperature	-10 .. +85	$^\circ\text{C}$	
T_S	Ambient storage temperature	-25 .. +100	$^\circ\text{C}$	
R_S	Secondary coil resistance @	$T_A = 70^\circ\text{C}$	43	Ω
		$T_A = 85^\circ\text{C}$	46	Ω
m	Mass	550	g	
		Standards	EN 50178: 1997	

Notes: ¹⁾ Pollution class 2. With a non insulated primary bar which fills the through-hole.

²⁾ With a di/dt of 100 A/ μs .

070807/7

Dimensions LT 1005-S (in mm. 1 mm = 0.0394 inch)



Mechanical characteristics

- General tolerance ± 0.5 mm
- Fastening 4 holes $\varnothing 6.5$ mm
- Primary through-hole 40.5 x 40.5 mm
- Connection of secondary Faston 6.3 x 0.8 mm

Remarks

- I_s is positive when I_p flows in the direction of the arrow.
- Temperature of the primary conductor should not exceed 100°C.
- Dynamic performances (di/dt and response time) are best with a single bar completely filling the primary hole.
- This is a standard model. For different versions (supply voltages, turns ratios, unidirectional measurements...), please contact us.



■ Features :

- Universal AC input/Full range
- Protections: Short circuit / Overload / Over voltage
- Cooling by free air convection
- Can be installed on DIN rail TS-35/7.5 or 15
- Class I, Div 2 Hazardous Locations T4
- LED indicator for power on
- DC OK relay contact
- No load power consumption<0.75W
- 100% full load burn-in test
- 3 years warranty



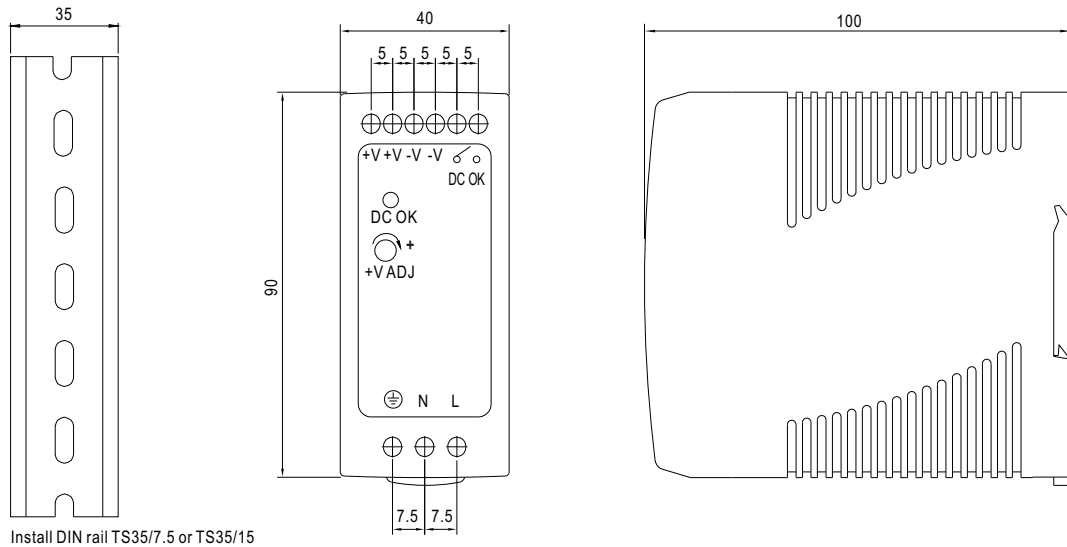
SPECIFICATION



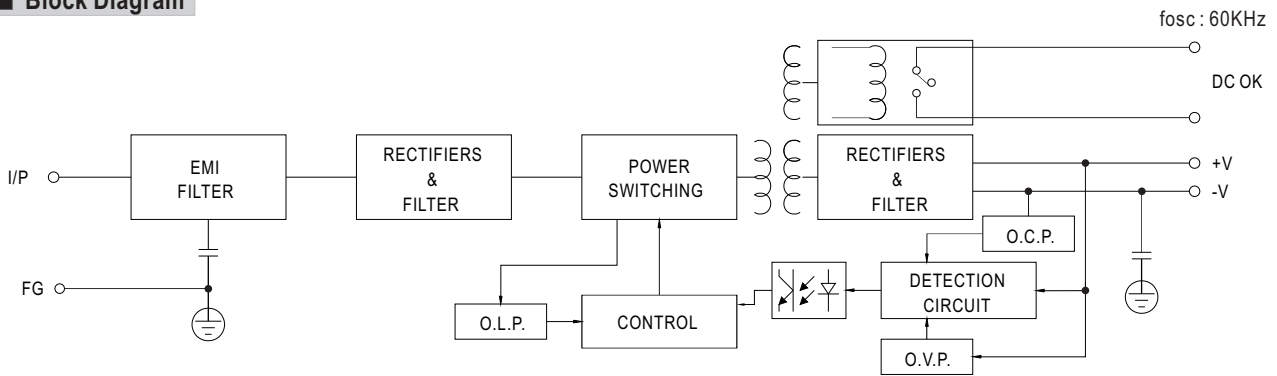
MODEL	MDR-60-5	MDR-60-12	MDR-60-24	MDR-60-48	
OUTPUT	DC VOLTAGE	5V	12V	24V	48V
	RATED CURRENT	10A	5A	2.5A	1.25A
	CURRENT RANGE	0 ~ 10A	0 ~ 5A	0 ~ 2.5A	0 ~ 1.25A
	RATED POWER	50W	60W	60W	60W
	RIPPLE & NOISE (max.) Note.2	80mVp-p	120mVp-p	150mVp-p	200mVp-p
	VOLTAGE ADJ. RANGE	5 ~ 6V	12 ~ 15V	24 ~ 30V	48 ~ 56V
	VOLTAGE TOLERANCE Note.3	±2.0%	±1.0%	±1.0%	±1.0%
	LINE REGULATION	±1.0%	±1.0%	±1.0%	±1.0%
	LOAD REGULATION	±1.5%	±1.0%	±1.0%	±1.0%
	SETUP, RISE TIME Note.5	500ms, 30ms/230VAC 500ms, 30ms/115VAC at full load			
HOLD UP TIME (Typ.)	50ms/230VAC 20ms/115VAC at full load				
INPUT	VOLTAGE RANGE	85 ~ 264VAC 120 ~ 370VDC			
	FREQUENCY RANGE	47 ~ 63Hz			
	EFFICIENCY (Typ.)	78%	86%	88%	87%
	AC CURRENT (Typ.)	1.8A/115VAC 1A/230VAC			
	INRUSH CURRENT (Typ.)	COLD START 30A/115VAC 60A/230VAC			
	LEAKAGE CURRENT	<1mA/ 240VAC			
PROTECTION	OVERLOAD	105 ~ 150% rated output power Protection type : Constant current limiting, recovers automatically after fault condition is removed			
	OVER VOLTAGE	6.25 ~ 7.25V	15.6 ~ 18V	31.2 ~ 36V	57.6 ~ 64.8V
		Protection type : Shut down o/p voltage, re-power on to recover			
FUNCTION	DC OK SIGNAL	Relay contact rating(max.): 30V/1A resistive			
ENVIRONMENT	WORKING TEMP.	-20 ~ +70°C (Refer to "Derating Curve")			
	WORKING HUMIDITY	20 ~ 90% RH non-condensing			
	STORAGE TEMP., HUMIDITY	-40 ~ +85°C, 10 ~ 95% RH			
	TEMP. COEFFICIENT	±0.03%/°C (0 ~ 50°C)			
	VIBRATION	Component : 10 ~ 500Hz, 2G 10min./1cycle, period for 60min. each along X, Y, Z axes ; Mounting : Compliance to IEC60068-2-6			
SAFETY & EMC (Note 4)	SAFETY STANDARDS	UL508, UL62368-1, TUV BS EN/EN62368-1, Class I, Div. 2 Group A, B, C, D Hazardous Locations T4, EAC TP TC 004, BSMI CNS14336-1, AS/NZS 60950.1, IS13252(Part1)/IEC60950-1approved			
	WITHSTAND VOLTAGE	I/P-O/P:3KVAC I/P-FG:2KVAC O/P-FG:0.5KVAC			
	ISOLATION RESISTANCE	I/P-O/P, I/P-FG, O/P-FG:>100M Ohms / 500VDC / 25°C / 70% RH			
	EMC EMISSION	Compliance to BS EN/EN55032 (CISPR32), BS EN/EN61204-3 Class B, BS EN/EN61000-3-2,-3, EAC TP TC 020, CNS13438 Class B			
	EMC IMMUNITY	Compliance to BS EN/EN61000-4-2, 3, 4, 5, 6, 8, 11, BS EN/EN55024, BS EN/EN61000-6-2, BS EN/EN61204-3, heavy industry level, criteria A, EAC TP TC 020			
OTHERS	MTBF	299.2K hrs min. MIL-HDBK-217F (25°C)			
	DIMENSION	40*90*100mm (W*H*D)			
	PACKING	0.33Kg; 42pcs/14.8Kg/0.82CUFT			
NOTE	<p>1. All parameters NOT specially mentioned are measured at 230VAC input, rated load and 25°C of ambient temperature.</p> <p>2. Ripple & noise are measured at 20MHz of bandwidth by using a 12" twisted pair-wire terminated with a 0.1uf & 47uf parallel capacitor.</p> <p>3. Tolerance : includes set up tolerance, line regulation and load regulation.</p> <p>4. The power supply is considered a component which will be installed into a final equipment. The final equipment must be re-confirmed that it still meets EMC directives. For guidance on how to perform these EMC tests, please refer to "EMI testing of component power supplies." (as available on http://www.meanwell.com)</p> <p>5. Length of set up time is measured at first cold start. Turning ON/OFF the power supply may lead to increase of the set up time.</p> <p>6. The ambient temperature derating of 3.5°C/1000m with fanless models and of 5°C/1000m with fan models for operating altitude higher than 2000m(6500ft).</p> <p>※ Product Liability Disclaimer : For detailed information, please refer to https://www.meanwell.com/serviceDisclaimer.aspx</p>				

Case No.962A Unit:mm

Mechanical Specification



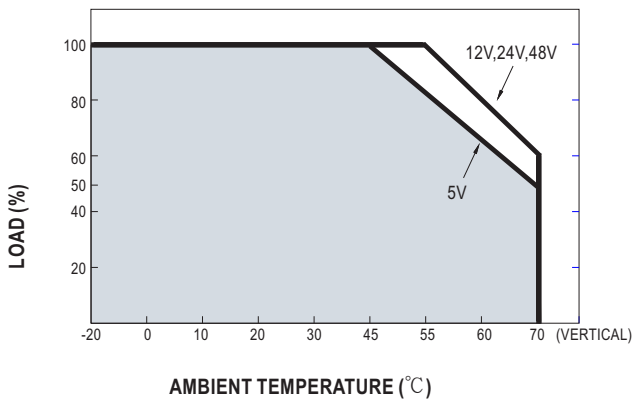
Block Diagram



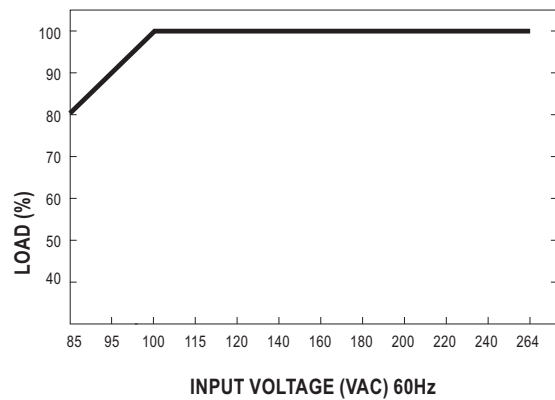
DC OK Relay Contact

Contact Close	PSU turns on / DC OK.
Contact Open	PSU turns off / DC Fail.
Contact Ratings (max.)	30V/1A resistive load.

Derating Curve





Output Derating VS Input Voltage





- + 4G LTE Cat.4 Industrial Router
- + 2× Micro SIM with cover
- + 2× Ethernet 10/100
- + *optional WiFi - 802.11b/g/n, AP, Multi SSID, WDS
- + *optional GNSS receiver
- + MicroSD card slot for System log
- + Metal cover with DIN and Wall mount options
- + WAN failover

ORDERING INFORMATION

MODEL NO. - ORDER CODES	REGION	2× ETHERNET	GNSS (ANT)	ANT + DIV	2× SIM	WI-FI 802.11b/g/n	MicroSD	R-SEENET	ACCESSORIES POWER SOURCE + ANT
 ICR-1601G	EMEA	✓	✓	✓	✓		✓	✓	✓
 ICR-1601W	EMEA	✓		✓	✓	✓	✓	✓	✓

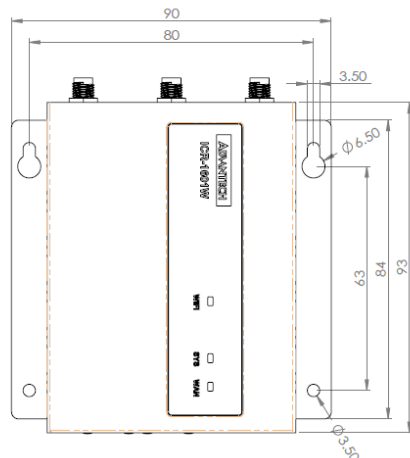
HARDWARE SPECIFICATIONS

PORTS, LED, ANTENNAS	
2× Ethernet	RJ45, 10/100 Mbps
2× SIM	SIMs Micro (3FF)
1× MicroSD	MicroSD card slot (System log)
LED indicators	WAN, System
2× ANT	SMA connectors
GNSS (GPS, GLONASS) - *optional	SMA connector
WiFi antenna - *optional	R-SMA connector
POWER, CONSUMPTION, ENVIRONMENTAL	
Power Supply	5–18VDC (DC Jack)
Consumption	7 W
Temperature Range – Operating / Storage	-30 to +70 °C / -40 to +85 °C
Humidity – Operating / Storage (non-condensing)	10 to 95 % / 10 to 95 %

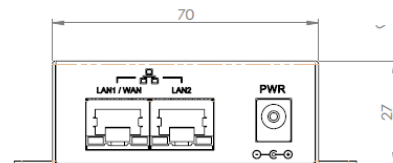
MECHANICAL	
Metal case	Wall mount & and DIN mount options
Enclosure Dimensions	93×90×27mm (100mm including antenna connectors)
Weight	252 g
WI-FI	
Antenna Connector	1× R-SMA – 50 Ohms
Supported WiFi band	2.4 GHz
Standards	802.11n, 802.11g, 802.11b
2.4 GHz supported channels	1, 2, 3, 4, 5, 6, 7, 8, 9, 10, 11, 12, 13
Functions	Multi-SSID, WMM, WDS
Security	WEP, WPA, WPA2, WPA-PSK, WPA2-PSK, 802.1x
Type of device	Access Point

MECHANICAL DRAWING

BOTTOM VIEW



FRONT VIEW



ICR-1601G/W

INDUSTRIAL CELLULAR 4G LTE Cat.4 ROUTER



SPECIFICATIONS - CONTINUED

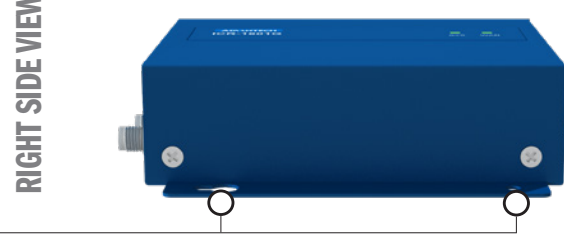
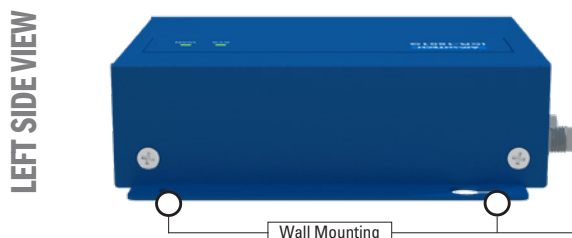
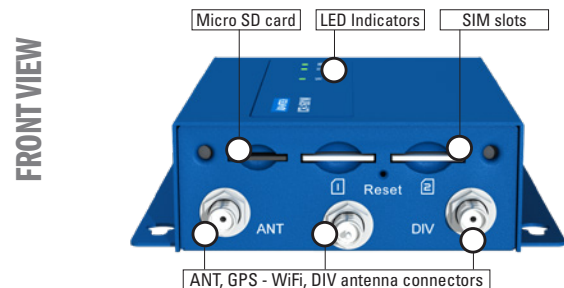
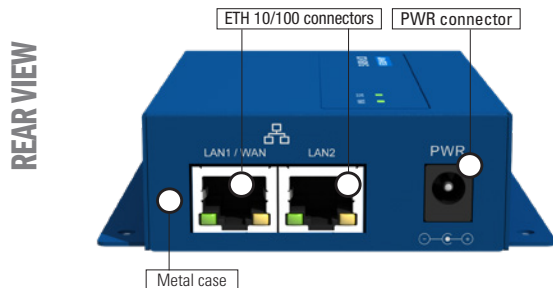
NETWORK FEATURES	
WAN & Uplink	WAN: Cellular, Ether-WAN, 1x config. 802.11n WiFi; Failover Cellular: 2G/3G/LTE, IP Pass-through, IPv4/v6 Ether-WAN: Dynamic IP, Static IP, PPPoE, PPTP, L2TP Network Monitor: ICMP/DNS Query
Networking	LAN & VLAN: DHCP Server/Relay, Port/Tag based VLAN IPv6*: Dual Stack, Static IPv6, DHCPv6, PPPoEv6 Port Forward: Virtual Server, Virtual Computer, DMZ, VPN Pass-through Routing: Static, Dynamic - RIP1/RIP2, OSPF, BGP
Object	Scheduling: Time Schedule List Ext. Server: Email, Syslog, RADIUS Certificate: My Certificate, Trusted Certificate, Issue Certificate
Security	VPN Tunneling: IPsec, OpenVPN, PPTP, L2TP, GRE VPN Capability: IPsec: up to 3 tunnels Firewall: SPI Firewall with Stealth Mode, IPS Access Control: Packet Filter, URL Blocking, MAC Filter
Administration	Config & Management: Web, Telnet & SSL, Command Script, SNMPv3 Std. & Proprietary MIB, TR069 System: Upgrade, Backup & Restore, Reboot & Reset, SysLog Diagnostic: Packet Analyzer, Diagnostic Tools
Service	Cellular Toolkit: Data Usage, SMS, SIM PIN, Network Scan Event Handling: User Defined Manage/Notify Event; SMS, Mail, Syslog, SNMP Trap System HW GNSS*: GPS Location Tracking / Viewer

CELLULAR MODULE PARAMETERS	
LTE parameters	LTE FDD Cat.4 Bit rate: 150 Mbps (DL) / 50 Mbps (UL) Supported frequencies: 800 MHz (B20), 900 MHz (B8), 1800 MHz (B3), 2100 MHz (B1), 2600 MHz (B7) Transmit power: 23±2.7 dBm
WCDMA parameters	Bit rate: 42.0 Mbps (DL) / 5.76 Mbps (UL) Supported frequencies: 900 MHz (B8), 2100 MHz (B1) Transmit power: 24+1/-3 dBm
GPRS/EDGE parameters	GPRS bit rate: 85.6 kbps (DL) / 85.6 kbps (UL) EDGE bit rate: 236.8 kbps (DL) / 236.8 kbps (UL) GPRS multislot class 10, EDGE multislot class 12 Supported frequencies: 900 MHz (B8), 1800 MHz (B3) GSM900 transmit power: 33±2 dBm GSM1800 transmit power: 30±2 dBm

ACCESSORIES - INCLUDED

ICR-1601G	ICR-1601W
Quick Start Guide	Quick Start Guide
2 x stick LTE antenna	2 x stick LTE antenna, 1 x stick WiFi antenna
Power adapter (5V DC/2A)	Power adapter (5V DC/2A)
DIN-rail bracket	DIN-rail bracket
Rubber feet	Rubber feet

INDUSTRY CERTIFICATIONS & APPROVALS ICR-1601	
EMC	EN 301 489-1 v 2.2.0, EN 301 489-3 v 2.1.1, EN 301 489-19 v 2.1.0, EN 301 489-52 v 1.1.0, EN 301 489-7 v 1.3.1, EN 301 489-24 v 1.5.1, EN 301 489-17 v 3.1.1
Radio	EN 301 511 v 12.5.1, EN 301 908-1 v 11.1.1, EN 301 908-2 v 11.1.1, EN 301 908-13 v 11.1.1, EN 303 413 v 1.1.1, EN 300 440 v 2.1.1, EN 300 328 v 2.1.1
Safety	EN 60 950-1, EN 62 368-1, EN 50 385, EN 62311
Environmental	RoHS, Reach, WEEE





- Low surface temperature**
- Integrated thermostat**
- Compact size**
- Wide voltage range**
- Double insulated protection**
- DIN rail mountable**

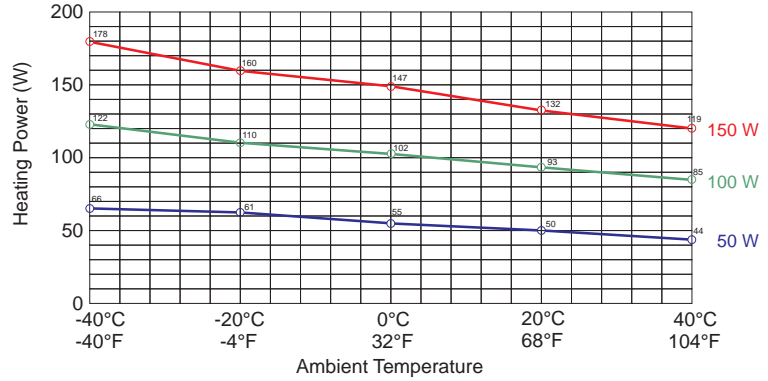
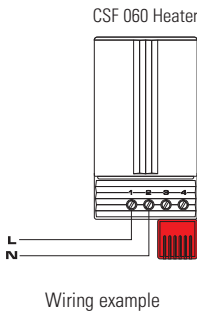
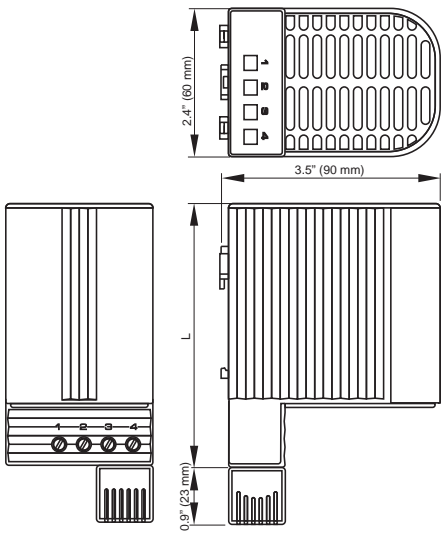
The CSF 060 is a touch-safe heater for use in enclosures. The design of the heater utilizes natural convection which results in a circulating current of warm air. The surface temperatures on the accessible side surfaces of the housing are minimized as a result of the heater design. This model with plug-in thermostat does not require additional wiring. The CSF 060 is also available in a version without thermostat (CS 060).



Technical Data

Operating voltage	120-240VAC* (min. 110V, max. 265V)
Heating capacity	see table
Heating element	PTC resistor - temperature limiting
Surface temperature	< 176°F (80°C), except upper protective grill
Connection	4-pole terminal AWG 14 max (2.5mm ²), torque 0.8Nm max.
Housing	plastic, UL 94V-0, black
Mounting	clip for 35mm DIN rail, EN 60 715
Mounting position	vertical
Operating / Storage temperature	-4 to +158°F (-20 to +70°C) / -49 to +158°F (-45 to +70°C)
Protection class	II (double insulated)
Protection type	IP 20
Approvals	UL File No. E150057, VDE

*Operating with voltages below 140VAC reduces heating performance by approx. 10%.



Part No.	Heating capacity ¹⁾	Max. current (inrush)	Air outlet temperature ²⁾	Switch-off temperature ³⁾	Switch-on temperature ³⁾	Dimensions	Weight (approx.)
06001.0-00	50W	2.5A	187°F (86°C)	59°F (15°C)	41°F (5°C)	5.2 x 2.4 x 3.5" (133 x 60 x 90mm)	10.6 oz. (300g)
06002.0-00	50W	2.5A	187°F (86°C)	77°F (25°C)	59°F (15°C)	5.2 x 2.4 x 3.5" (133 x 60 x 90mm)	10.6 oz. (300g)
06011.0-00	100W	4.5A	248°F (120°C)	59°F (15°C)	41°F (5°C)	5.2 x 2.4 x 3.5" (133 x 60 x 90mm)	10.9 oz. (310g)
06012.0-00	100W	4.5A	248°F (120°C)	77°F (25°C)	59°F (15°C)	5.2 x 2.4 x 3.5" (133 x 60 x 90mm)	10.9 oz. (310g)
06021.0-00	150W	8.0A	293°F (145°C)	59°F (15°C)	41°F (5°C)	6.8 x 2.4 x 3.5" (173 x 60 x 90mm)	15.5 oz. (440g)
06022.0-00	150W	8.0A	293°F (145°C)	77°F (25°C)	59°F (15°C)	6.8 x 2.4 x 3.5" (173 x 60 x 90mm)	15.5 oz. (440g)

¹⁾ see Heating capacity / Ambient temperature diagram
²⁾ measured 2" (50mm) above protective grill
³⁾ tolerance of ± 5K

Specifications are subject to change without notice. Suitability of this product for its intended use and any associated risks must be determined by the end customer/ buyer in its final application.

SMALL COMPACT THERMOSTAT

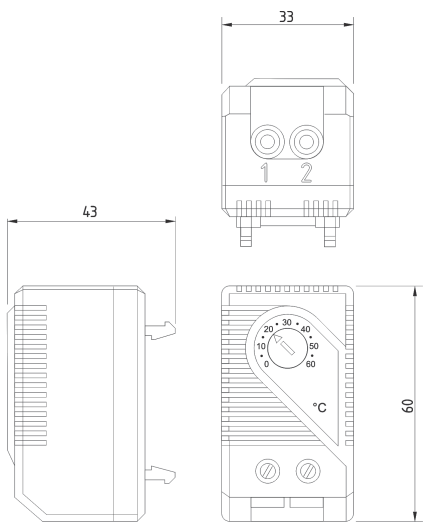
KTO 011 / KTS 011



- > Large setting range
- > Small size
- > Simple to mount
- > High switching performance

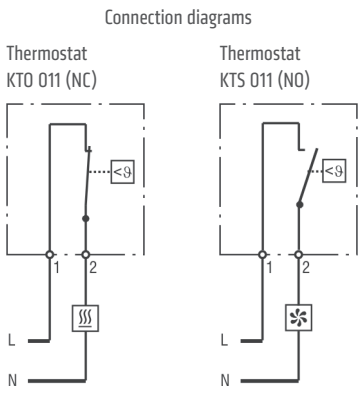
KTO 011: Thermostat (normally closed); contact breaker for regulating heaters. The contact opens when temperature is rising.

KTS 011: Thermostat (normally open); contact maker for regulating of filter fans and heat exchangers or for switching signal devices when temperature limit has been exceeded. The contact closes when temperature is rising.



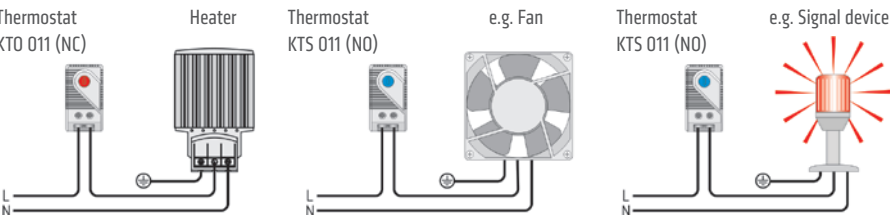
TECHNICAL DATA

Switch temperature difference	7K (±4K tolerance)
Sensor element	thermostatic bimetal
Contact type	snap-action contact
Service life	> 100,000 cycles
Max. switching capacity	250VAC, 10 (2) A 120VAC, 15 (2) A DC 30W at 24VDC to 72VDC
Max. inrush current	AC 16A for 10 sec.
Connection ¹	2-pole terminal, clamping torque 0.5Nm max.: rigid wire 2.5mm ² , stranded wire (with wire end ferrule) 1.5mm ²
Mounting	clip for 35mm DIN rail, EN 60715
Casing	plastic according to UL94 V-0, light grey
Dimensions	60 x 33 x 43mm
Weight	approx. 40g
Fitting position	variable
Operating/Storage temperature	-45 to +80°C (-49 to +176°F)
Operating/Storage humidity	max. 95% RH (non-condensing)
Protection type	IP20



- Heater
- Filter fan, Cooling equipment, Signal device

¹ When connecting with wires, wire end ferrules must be used.
Important note: The contact system of the regulator is subjected to environmental influences, thus the contact resistance may change. This can lead to a voltage drop and/or self-heating of the contacts.



Setting range	Art. No. Contact breaker (NC)	Art. No. Contact maker (NO)	Approvals			
0 to +60°C	01140.0-00	01141.0-00	VDE	-	-	EAC
-10 to +50°C	01142.0-00	01143.0-00	VDE	UL File No. E164102	-	EAC
+20 to +80°C	01159.0-00	01158.0-00	VDE	UL File No. E164102	CSA	EAC
+32 to +140°F	01140.9-00	01141.9-00	VDE	UL File No. E164102	CSA	EAC
+14 to +122°F	01142.9-00	01143.9-00	VDE	UL File No. E164102	CSA	EAC
0 to +60°C	01146.9-00	01147.9-00	VDE	UL File No. E164102	CSA	EAC

Caravan/Boat Package



- SmartDisc hole mounted antenna for Rugged installations – IP67
- Operable in 2G/3G/4G
- Smart choice for mounting on Boats, caravans etc
- Groundplane independent
- 2,5meter white cable SMA-male (suitable for most routers)
- Adapter for CRC-9 and TS-9 included (common connection for USB-modems)
- Frequency range 880-960/1710-2690 MHz
- 2,15 dBi typical gain
- Article no: 710123



Note: Modem not included



34970A Data Acquisition/ Switch Unit Family

34970A

34972A

Notice: The 34972A will be discontinued on June 1, 2020. The last day to place order for this product is May 31, 2020. Keysight will continue to provide world-class support for this product for the standard period of 5 years.



At a fraction of the cost of other standalone data acquisition systems

- 3-slot mainframe with built-in 6½ digit DMM and
- 8 optional switch and control plug-in modules
- Measures and converts 11 different input signals: temperature with thermocouples, RTDs and thermistors; dc/ac volts; 2- and 4-wire resistance; frequency and period; dc/ac current
- IO options for easy connectivity to your PC:
- 34970A: GPIB, RS-232
- 34972A: LAN, USB
- Graphical Web interface for point and click monitor and control (34972A)
- USB flash drive support to copy/log data in standalone applications (34972A)
- Includes BenchVue DAQ software to configure and control tests, display results and collect data for further analysis

Table of Contents

Features	03
More Power and Flexibility than You Ever Imagined You Could Afford	06
The Keysight 34970A/34972A Offers Unequaled Versatility for Your Data Acquisition Applications	07
A powerful, flexible data acquisition system for automated test.....	10
ATE feature checklist	11
Low-cost, high-quality switching for automated test	12
Customize your Keysight 34970A/34972A with plug-in modules	13
34970A and 34972A Keysight modules-at-a-glance selection guide.....	13
Keysight Quality	14
Spec Interpretation Guide	15
34970A/34972A Accuracy Specifications ±(% of reading + % of range)	16
Single Channel Reading Rates to I/O or Internal Memory.....	18
System Specifications	19
Modules Specifications.....	20
Multiplexer Selection Guide	21
34901A.....	21
34902A	22
34908A	22
34903A	23
34904A	23
34905A 50 Ω/34906A 75 Ω	24
34907A	25
Rack Mounting and Dimensions.....	26
Ordering Information.....	27

Customize your Keysight 34970A/34972A with plug-in modules

A complete selection of plug-in modules gives you high quality measurement, switching, and control capabilities to choose from. Modules include both low-frequency and RF multiplexers, a matrix switch, a general-purpose switch, and a multifunction module that includes digital input/output, analog output, and totalizer capabilities. You can mix and match modules to get just the functionality you need right now—then change or add more channels later as your application grows.

Modules for the 34970A/34972A are designed to make your testing easier, faster, and more reliable. Here's how:

Higher throughput

Our unique architecture incorporates a high-performance microprocessor on each module, off loading the mainframe processor and minimizing backplane communications for faster throughput.

More channels in less space

Surface mount construction and a highly integrated design minimize the space required for relay drive and interface circuitry. High density on-module connectors save both board and connector space normally required by a terminal block. We use the latest technology to squeeze the most out of the remaining board space, giving you up to 40 single-ended channels in roughly the same space used by many data acquisition system terminal blocks.

Convenient connections

On-module screw-terminal connectors make wiring more convenient. Built-in strain relief cable routing and cable tie points keep your wiring secure and safe from accidental tugs and pulls. An internal analog bus routes signals from any of the low frequency multiplexers directly to the internal DMM, without the need for external connections.

Use the chart below to help you pinpoint the modules that meet your needs.

34970A and 34972A Keysight modules-at-a-glance selection guide

Model description	Type	Speed (ch/sec)	Max volts	Max amps	Bandwidth	Thermal offset	Comments	Page
34901A 20 ch Multiplexer + 2 current channels	2-wire armature (4-wire selectable)	60	300 V	1 A	10 MHz	< 3 μ V	Built-in cold junction reference 2 additional current channels (22 total)	21
34902A 16 ch Multiplexer	2-wire reed (4-wire selectable)	250 ^[1]	300 V	50 mA	10 MHz	< 6 μ V	Built-in cold junction reference	21
34903A 20 ch Actuator/GP Switch	SPDT/form C	120	300 V	1 A	10 MHz	< 3 μ V		23
34904A 4 x 8 Matrix	2-wire armature	120	300 V	1 A	10 MHz	< 3 μ V		23
34905A Dual 4 ch RF Mux 50 Ω	Common low (unterminated)	60	42 V	0.7 A	2 GHz	< 6 μ V	1 GHz bandwidth through BNC-to-SMB adapter cable	24
34906A Dual 4 ch RF Mux 75 Ω	Common low (unterminated)	60	42 V	0.7 A	2 GHz	< 6 μ V	1 GHz bandwidth through BNC-to-SMB adapter cable	24
34907A Multifunction Module	Two 8-bit digital I/O ports		42 V	400 mA			Open drain	25
	26-bit event counter		42 V		100 KHz		Selectable input threshold	
	Two 16-bit analog outputs		\pm 12 V	10 mA	dc		Max 40 mA total output per frame	
34908A 40 ch Single-Ended Mux	1-wire armature (common low)	60	300 V	1A	10 MHz	< 3 μ V	Built-in cold junction reference No four-wire measurements	21

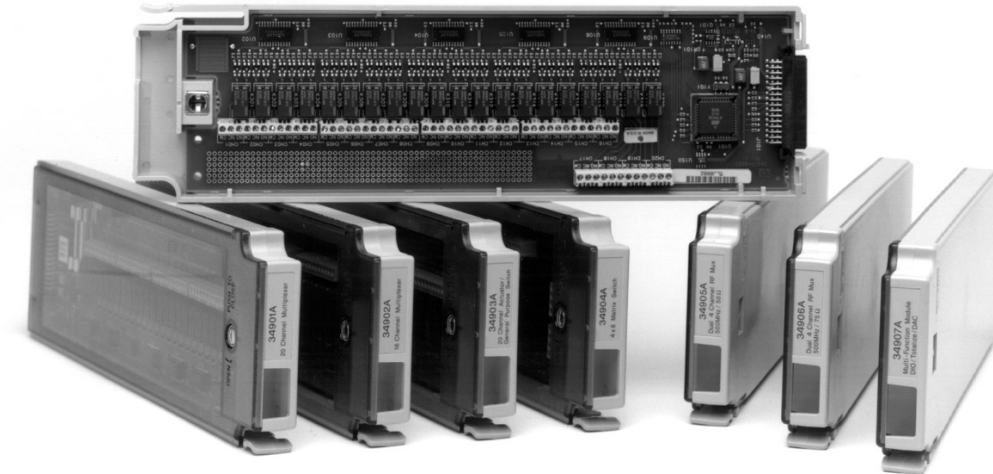
[1] Up to 250 ch/sec to internal memory.
See scanning rates for measurement condition and rate on each instrument.

Keysight quality

We know you can't afford instrument downtime due to hardware failures and unscheduled maintenance. That's why our engineers designed reliability into the 34970A/34972A: A rugged enclosure, state-of-the-art surface mount construction throughout, reduced parts counts, and rigorous and thorough testing on all aspects of the product.

Take the guesswork out of relay maintenance

The 34970A/34972A uses our proprietary relay maintenance system to help you to predict relay end-of-life and avoid costly production line downtime. It automatically counts every individual switch closure and stores it in nonvolatile memory on each module. You can query the total number of cycles on any individual channel so you can schedule maintenance and avoid erratic end-of-life failures.



Spec interpretation guide

The following pages list the technical specifications for the Keysight 34970A/34972A Data Acquisition/Switch Unit and its modules. The explanations and examples below are helpful in understanding how to interpret these specifications:

- Measurement accuracy is specified as percent of reading plus percent of range, where reading is the actual measured value and range is the name of the scale (1 V, 10 V, etc.)—not the full scale value (1.2 V, 12 V, etc.).
- DMM measurement accuracies include all switching errors. Switching errors are also listed separately in the module specifications section. Temperature measurement accuracies include ITS-90 conversion errors. The thermocouple accuracies include the reference junction error as well.
- Accuracies are listed as either 24-hour, 90-day, or 1-year specifications. This refers to the length of time since the instrument's last calibration. Use the specification that matches your calibration cycle. The 24-hour specifications are useful for determining short-term relative performance.

Example 1: Basic dcV accuracy

Calculate the accuracy of the following measurement:

9 V dc input
10 V dc range
1-year accuracy specifications
Normal operating temperature (18 - 28°C)

From the following page, the 1-year accuracy is:
0.0035% of reading + 0.0005% of range

Which translates into:
 $(0.0035/100 \times 9 \text{ V}) + (0.0005/100 \times 10 \text{ V}) = 365 \mu\text{V}$

For a total accuracy of:
 $365 \mu\text{V}/9 \text{ V} = 0.0041\%$

Example 2: Extreme operating temperature

When the 34970A/34972A is used outside of its 18 - 28°C temperature range, there are additional temperature drift errors to consider. Assume the same conditions in Example 1, but at a 35°C operating temperature.

The basic accuracy is again:
0.0035% of reading + 0.0005% of range = 365 μV .

Now, multiply the 10 V temperature coefficient from the following page by the number of degrees outside of operating range for additional error:

$(0.0005\% \text{ reading} + 0.0001\% \text{ range})$
 $/^\circ\text{C} \times (35 - 28^\circ\text{C}) =$
 $(0.0005\% \text{ reading} + 0.0001\% \text{ range})$
 $/^\circ\text{C} \times 7^\circ\text{C} =$

0.0035% reading + 0.0007% range = 385 μV

Total error is then:

365 μV + 385 μV = 750 μV or 0.008%

Example 3: Thermocouple measurement accuracy

Calculating the total thermocouple reading error is easy with the 34970A/34972A—just add the listed measurement accuracy to the accuracy of your transducer. Switching, conversion, and reference junction errors are already included in the measurement specification. For this example, assume a J-type thermocouple input reading 150°C.

From the following page, total error is:
Thermocouple probe accuracy + 1.0°C
The probe vendor specifies accuracy of 1.1°C
or 0.4%, whichever is greater.

Total error is then:

1.0°C + 1.1°C = 2.1°C total, or 1.4%

Example 4: acV accuracy

The acV function measures the true RMS value of the input waveform, regardless of waveshape. Listed accuracies assume a sinewave input. To adjust accuracies for non-sinusoids, use the listed crest factor adder.

For this example, assume a $\pm 1 \text{ V}$ square wave input with 50% duty cycle and a 1 kHz frequency.

Accuracy for 1 V, 1 kHz sinusoid is:

0.06% reading + 0.04% range

A 50% duty cycle squarewave has a crest factor of

Peak value / RMS value = 1 V / 1 V = 1

From crest factor table, add:

0.05% of reading

The total accuracy is:

0.11% of reading + 0.04% of range = 1.5 mV or 0.15%

34970A/34972A accuracy specifications \pm (% of reading + % of range)^[1]

Includes measurement error, switching error, and transducer conversion error

	Range ^[3]	Frequency, etc.	24 hour ^[2] 23 \pm 1°C	90 Day 23 \pm 5°C	1 Year 23 \pm 5°C	Temperature coefficient 0 - 18°C, 28 - 55°C
DC voltage						
	100.0000 mV		0.0030 + 0.0035	0.0040 + 0.0040	0.0050 + 0.0040	0.0005 + 0.0005
	1.000000 V		0.0020 + 0.0006	0.0030 + 0.0007	0.0040 + 0.0007	0.0005 + 0.0001
	10.00000 V		0.0015 + 0.0004	0.0020 + 0.0005	0.0035 + 0.0005	0.0005 + 0.0001
	100.0000 V		0.0020 + 0.0006	0.0035 + 0.0006	0.0045 + 0.0006	0.0005 + 0.0001
	300.000 V		0.0020 + 0.0020	0.0035 + 0.0030	0.0045 + 0.0030	0.0005 + 0.0003
True RMS AC voltage ^[4]						
	All ranges from 100.0000 mV to 100.0000 V	3 Hz-5 Hz	1.00 + 0.03	1.00 + 0.04	1.00 + 0.04	0.100 + 0.004
		5 Hz-10 Hz	0.35 + 0.03	0.35 + 0.04	0.35 + 0.04	0.035 + 0.004
		10 Hz-20 kHz	0.04 + 0.03	0.05 + 0.04	0.06 + 0.04	0.005 + 0.004
		20 kHz-50 kHz	0.10 + 0.05	0.11 + 0.05	0.12 + 0.05	0.011 + 0.005
		50 kHz-100 kHz	0.55 + 0.08	0.60 + 0.08	0.60 + 0.08	0.060 + 0.008
	300.0000 V	100 kHz-300 kHz ^[5]	4.00 + 0.50	4.00 + 0.50	4.00 + 0.50	0.20 + 0.02
		3 Hz-5 Hz	1.00 + 0.05	1.00 + 0.08	1.00 + 0.08	0.100 + 0.008
		5 Hz-10 Hz	0.35 + 0.05	0.35 + 0.08	0.35 + 0.08	0.035 + 0.008
		10 Hz-20 kHz	0.04 + 0.05	0.05 + 0.08	0.06 + 0.08	0.005 + 0.008
		20 kHz-50 kHz	0.10 + 0.10	0.11 + 0.12	0.12 + 0.12	0.011 + 0.012
	50 kHz-100 kHz	50 kHz-100 kHz	0.55 + 0.20	0.60 + 0.20	0.60 + 0.20	0.060 + 0.020
		100 kHz-300 kHz ^[5]	4.00 + 1.25	4.00 + 1.25	4.00 + 1.25	0.20 + 0.05
		100 kHz-300 kHz ^[5]	4.00 + 1.25	4.00 + 1.25	4.00 + 1.25	0.20 + 0.05
Resistance ^[6]						
	100.0000 Ω	1 mA current source	0.0030 + 0.0035	0.008 + 0.004	0.010 + 0.004	0.0006 + 0.0005
	1.000000 k Ω	1 mA	0.0020 + 0.0006	0.008 + 0.001	0.010 + 0.001	0.0006 + 0.0001
	10.00000 k Ω	100 μ A	0.0020 + 0.0005	0.008 + 0.001	0.010 + 0.001	0.0006 + 0.0001
	100.0000 k Ω	10 μ A	0.0020 + 0.0005	0.008 + 0.001	0.010 + 0.001	0.0006 + 0.0001
	1.000000 M Ω	5.0 μ A	0.002 + 0.001	0.008 + 0.001	0.010 + 0.001	0.0010 + 0.0002
	10.00000 M Ω	500 nA	0.015 + 0.001	0.020 + 0.001	0.040 + 0.001	0.0030 + 0.0004
	100.0000 M Ω	500 nA 10 M Ω	0.300 + 0.010	0.800 + 0.010	0.800 + 0.010	0.1500 + 0.0002
Frequency and period ^[7]						
	100 mV to 300V	3 Hz-5 Hz	0.10	0.10	0.10	0.005
		5 Hz-10 Hz	0.05	0.05	0.05	0.005
		10 Hz-40 Hz	0.03	0.03	0.03	0.001
		40 Hz-300 kHz	0.006	0.01	0.01	0.001
DC current (34901A only)						
	10.00000 mA	<0.1 V burden	0.005 + 0.010	0.030 + 0.020	0.050 + 0.020	0.002 + 0.0020
	100.0000 mA	<0.6 V	0.010 + 0.004	0.030 + 0.005	0.050 + 0.005	0.002 + 0.0005
	1.000000 A	<2 V	0.050 + 0.006	0.080 + 0.010	0.100 + 0.010	0.005 + 0.0010
True RMS AC current (34901A only)						
	10.00000 mA and ^[4] 1.000000 A	3 Hz-5 Hz	1.00 + 0.04	1.00 + 0.04	1.00 + 0.04	0.100 + 0.006
		5 Hz-10 Hz	0.30 + 0.04	0.30 + 0.04	0.30 + 0.04	0.035 + 0.006
		10 Hz-5 kHz	0.10 + 0.04	0.10 + 0.04	0.10 + 0.04	0.015 + 0.006
	100.0000 mA ^[8]	3 Hz-5 Hz	1.00 + 0.5	1.00 + 0.5	1.00 + 0.5	0.100 + 0.06
		5 Hz-10 Hz	0.30 + 0.5	0.30 + 0.5	0.30 + 0.5	0.035 + 0.06
		10 Hz-5 kHz	0.10 + 0.5	0.10 + 0.5	0.10 + 0.5	0.015 + 0.06
Temperature						
Thermocouple ^[10]	Type	1-year accuracy ^[9]	1-year accuracy ^[9]	Extended range 1-year accuracy ^[9]	Temp coefficient/$^{\circ}$C	
	B	1100 to 1820 $^{\circ}$ C	1.2 $^{\circ}$ C	400 to 1100 $^{\circ}$ C	1.8 $^{\circ}$ C	
	E	-150 to 1000 $^{\circ}$ C	1.0 $^{\circ}$ C	-200 to -150 $^{\circ}$ C	1.5 $^{\circ}$ C	
	J	-150 to 1200 $^{\circ}$ C	1.0 $^{\circ}$ C	-210 to -150 $^{\circ}$ C	1.2 $^{\circ}$ C	
	K	-100 to 1200 $^{\circ}$ C	1.0 $^{\circ}$ C	-200 to -100 $^{\circ}$ C	1.5 $^{\circ}$ C	
	N	-100 to 1300 $^{\circ}$ C	1.0 $^{\circ}$ C	-200 to -100 $^{\circ}$ C	1.5 $^{\circ}$ C	0.03 $^{\circ}$ C
	R	300 to 1760 $^{\circ}$ C	1.2 $^{\circ}$ C	-50 to 300 $^{\circ}$ C	1.8 $^{\circ}$ C	
	S	400 to 1760 $^{\circ}$ C	1.2 $^{\circ}$ C	-50 to 400 $^{\circ}$ C	1.8 $^{\circ}$ C	
	T	-100 to 400 $^{\circ}$ C	1.0 $^{\circ}$ C	-200 to -100 $^{\circ}$ C	1.5 $^{\circ}$ C	
RTD	R0 from 49 Ω to 2.1 k Ω	-200 to 600 $^{\circ}$ C	0.06 $^{\circ}$ C			0.003 $^{\circ}$ C
Thermistor	2.2 k, 5 k, 10 k	-80 to 150 $^{\circ}$ C	0.08 $^{\circ}$ C			0.002 $^{\circ}$ C

- [1] Specifications are for 1 hr warm-up and 6½ digits, Slow ac filter
 [2] Relative to calibration standards
 [3] 20% over range on all ranges except 300 Vdc and ac ranges and 1 Adc and ac current ranges
 [4] For sinewave input > 5% of range. For inputs from 1% to 5% of range and < 50 kHz, add 0.1% of range additional error
 [5] Typically 30% of reading error at 1 MHz, limited to 1 x 108 V Hz

- [6] Specifications are for 4-wire ohms function or 2-wire ohms using scaling to remove the offset. Without scaling, add 4 Ω additional error in 2-wire Ohms function
 [7] Input > 100 mV. For 10 mV to 100 mV inputs multiply % of reading error x 10
 [8] Specified only for inputs >10 mA
 [9] For total measurement accuracy, add temperature probe error
 [10] Thermocouple specifications not guaranteed when 34907A module is present. For < 1 $^{\circ}$ C accuracy, a precision external reference is required.